

# Asymptotic Coincidence of the Statistics for Degenerate and Non-Degenerate Correlated Real Wishart Ensembles

Tim Wirtz,<sup>1,2,\*</sup> Mario Kieburg,<sup>1,3,†</sup> and Thomas Guhr<sup>1,‡</sup>

<sup>1</sup>*Fakultät für Physik, Universität Duisburg–Essen, Duisburg, Germany*

<sup>2</sup>*Fraunhofer Institut für Intelligente Analyse- und Informationssysteme, Sankt Augustin, Germany*

<sup>3</sup>*Fakultät für Physik, Universität Bielefeld, Bielefeld, Germany*

(Dated: December 7, 2024)

The correlated Wishart model provides the standard benchmark when analyzing time series of any kind. Unfortunately, the real case, which is the most relevant one in applications, poses serious challenges for analytical calculations. Often these challenges are due to square root singularities which cannot be handled using common random matrix techniques. We present a new way to tackle this issue. Using supersymmetry, we carry out an analytical study which we support by numerical simulations. For large but finite matrix dimensions, we show that statistical properties of the fully correlated real Wishart model generically approach those of a correlated real Wishart model with doubled matrix dimensions and doubly degenerate empirical eigenvalues. This holds for the local and global spectral statistics. With Monte Carlo simulations we show that this is even approximately true for small matrix dimensions. We explicitly investigate the  $k$ -point correlation function as well as the distribution of the largest eigenvalue for which we find a surprisingly compact formula in the doubly degenerate case. Moreover we show that on the local scale the  $k$ -point correlation function exhibits the sine and the Airy kernel in the bulk and at the soft edges, respectively. We also address the positions and the fluctuations of the possible outliers in the data.

PACS numbers: 05.45.Tp, 02.50.-r, 02.20.-a

## I. INTRODUCTION

Random matrix theory was first introduced in biostatistics by Wishart [1] and later on also by Wigner in the context of Hamiltonian systems [2, 3]. It has extraordinary power to model and study generic features in a variety of systems, see Ref. [4]. It only employs basis invariance and global symmetries of the matrices resulting in the orthogonal, unitary and symplectic ensembles [5]. Wishart's ideas opened a new direction in time series analysis and statistical inference [6–9, 15]. The Wishart model is widely used, including applications in fields such as medicine [10], biophysics [11], chemistry [12], finance [13, 14], wireless communication [16], to mention just a few. The Wishart model shares the unique advantage of all random matrix approaches: Most of its predictions are accessible in experiments or observations and can therefore directly be tested. Although the random matrix theory setup is straightforward, calculations are often difficult. The real case which is the most relevant one for applications is particularly cumbersome.

We thus focus on the case of  $p \times n$  rectangular matrices  $W$  with real entries  $W_{j\nu} \in \mathbb{R}$  for  $j = 1, \dots, p$  and  $\nu = 1, \dots, n$ . The  $p$  rows of  $W$  may be viewed as model time series of length  $n$ . We assume a Gaussian distribution [6, 7],

$$P(W|C) \sim \exp\left(-\frac{n}{2} \text{tr} WW^T C^{-1}\right), \quad (1)$$

where the  $p \times p$  matrix  $C$  is the empirical correlation matrix specific for the data under consideration. This matrix is input of the model and requires to be real symmetric with positive eigenvalues  $\Lambda_i$ ,  $i = 1, \dots, p$ . In particular we have  $C = V\Lambda V^T$  with  $V \in O(p)$  and  $\Lambda = \text{diag}(\Lambda_1, \dots, \Lambda_p)$ . The positive definite  $p \times p$  matrix  $WW^T$  is the model correlation matrix and due to our choice of  $P(W|C)$ , it is on average  $\langle WW^T \rangle = C$ .

In applications of the real Wishart model, correlated or not, square roots of characteristic polynomials and therefore branch cuts arise. For instance, gap probabilities related to the smallest and largest eigenvalue were found to possess a representation as averaged products of determinants in the denominator to half integer power [17]. Other examples are the eigenvalue density in the ordinary and doubly correlated Wishart model [18–21], the distribution of the smallest eigenvalue [22–25] as well as universality considerations in scattering theory [26, 27]. Those square roots are serious

---

\*tim.wirtz@iaais.fraunhofer.de

†kieburg@physik.uni-bielefeld.de

‡thomas.guhr@uni-due.de

obstacles in analytical calculations and a solution is urgently called for. To the best of our knowledge a comprehensive analytical strategy for averages over a product of characteristic polynomials to half integer power does not exist. For certain special cases some solutions are known [24, 25, 27].

The analytical calculations drastically simplify in the case that the empirical correlation matrix becomes doubly degenerate, because the square roots are not present anymore. Although this case is empirically rarely justified, our results provide very good approximations for the case without such degeneracies. Our main goal is a general approach to eigenvalue statistics in the real correlated Wishart model, which to some extent outmanoeuvres the square roots of characteristic polynomials such that standard random matrix techniques apply. Based on analytical calculations using supersymmetry [28, 29] and on numerical simulations we verify that most of the statistical properties in the bulk, at the edges and for the outliers of an arbitrary, correlated real Wishart ensemble do not depend on the degree of the degeneracy of the empirical correlation matrix. In particular, the spectral observables of a  $p \times n$  random matrix  $W$  correlated with  $C$  coincide with those of a  $lp \times ln$  random matrix correlated with  $C \otimes \mathbb{1}_l$  where  $l \in \mathbb{N}$  is the degree of degeneracy and  $\mathbb{1}_l$  is the  $l$ -dimensional identity matrix. This statement becomes exact for

$$0 < \frac{p}{n} = \gamma^2 < 1 \ll n, p \rightarrow \infty \quad (2)$$

under very moderate assumptions on the empirical correlation matrix  $C$ . The eigenvalue density of correlated Wishart ensembles with non-degenerate spectrum was already studied by many other in [30–33]. We will regain their results and additionally we derive results about the local spectral statistics.

As a by-product we also derive the sine and the Airy kernel for real matrices in the bulk and at the soft edges, respectively, for the fully correlated case. Importantly, we properly account for all Efetov–Wegner boundary contributions [34–36] which often pose substantial difficulties in supersymmetry calculations. To this end we apply Rothstein’s theory [37] and identify the results with those for the Gaussian Orthogonal Ensemble (GOE). We include outliers and discuss their positions and fluctuations, provided they are well-separated from all other eigenvalues.

We show that most of the spectral observables are independent of the degree of degeneracy, and we thus claim that the distributions of the largest eigenvalue for the correlated real Wishart ensembles with the empirical correlation matrices  $C$  and  $C \otimes \mathbb{1}_2$  are approximately equal in the limit of large matrix dimensions  $p$  and  $n$ . We derive a representation of the cumulative density function in terms of a  $p \times p$  Pfaffian ( $p$  even) for the  $2p \times 2n$  Wishart ensemble with  $C \otimes \mathbb{1}_2$ . For this purpose we start from an earlier result [17] and employ skew-orthogonal polynomials [38].

Although the results are derived in an asymptotic limit, we find surprisingly good agreement with numerical simulations already for rather small matrix dimensions. This allows a quantitative as well as a qualitative spectral analysis in the Wishart model without doubly degenerate empirical eigenvalues if  $p/n \sim \mathcal{O}(1)$  and  $n, p$  large.

Our study is structured as follows. In section II, we summarize the basics of the  $k$ -point function and present the corresponding supermatrix model. We also discuss the conditions on  $C$  to ensure that the limit  $n, p \rightarrow \infty$  with  $p/n \in [0, 1]$  is well-defined. The saddle point approximation of the supermatrix model is performed in section III in which we also derive a simple general relation between the macroscopic level density (marginal density) and the saddle point solution. Furthermore, we study the bulk and the edges of the spectrum and derive the sine kernel on the local scale. In section IV we investigate possible outliers and the local statistics of the soft edges and derive the Airy kernel. We also manage to express the cumulative distribution of the largest eigenvalue in terms of a Pfaffian determinant. For illustrating purpose and to confirm our claims, we perform numerical simulations in section V. We conclude in section VI. A brief sketch of Rothstein’s theory [37] is relegated to appendix A.

## II. SUPERSYMMETRIC REPRESENTATION OF THE $k$ -POINT CORRELATION FUNCTIONS

The  $k$ -point correlation function  $R_k(x; \xi)$  with  $k \leq p$  measures the eigenvalue fluctuations of the model correlation matrix  $WW^T$ . We use two sets of variables  $x = \text{diag}(x_1, \dots, x_k)$  and  $\xi = \text{diag}(\xi_1, \dots, \xi_k)$  for later separation of the global and the local scales, respectively. To study the local scale, we unfold the spectrum with the level density which depends on the empirical eigenvalues  $\Lambda = \text{diag}(\Lambda_1, \dots, \Lambda_p)$ . Importantly, on the original and on the unfolded scale, all  $k$ -point functions may depend non-trivially on these empirical eigenvalues. One of the main results to be derived below is the emergence of the universal statistical features of the *uncorrelated* Wishart ensemble after unfolding and under modest conditions on  $\Lambda$ . Furthermore, an arbitrary degeneracy of degree  $l \in \mathbb{N}$  of the empirical eigenvalues  $\Lambda \rightarrow \Lambda \otimes \mathbb{1}_l$  does not change the statistics. Even the global level density  $R_1(x)$  remains the same for large matrix dimensions  $n, p \rightarrow \infty$ . In sections II A and II B we set up the supermatrix model and test the asymptotics, respectively.

### A. Setting up the supermatrix model

To be as general as possible, we consider an ensemble of Wishart matrices  $W$  of size  $lp \times ln$  drawn from the normal distribution (1), where the eigenvalues of  $C$  are  $l$ -fold degenerate, *i.e.* the empirical eigenvalues are  $\Lambda \otimes \mathbb{1}_l$ . For this ensemble we analyze its  $k$ -point correlation function which is expressed as the derivative of a generating function,

$$R_k(x; \xi) = \frac{1}{(4\pi l)^k (lp)^k} \sum_{L \in \{\pm 1\}^k} \prod_{i=1}^k L_i \partial_{j_i} Z_{k,k}^{(p,n)}(\kappa) \Big|_{\substack{\varepsilon \rightarrow 0 \\ j=0}}, \quad (3)$$

where  $\kappa_{b,1} = x_b + j_b + \xi_b/(lp) + lL_b\varepsilon$ ,  $\kappa_{b,2} = x_b - j_b + \xi_b/(lp) + lL_b\varepsilon$  and  $L_b = \pm 1$  for  $b = 1, \dots, k$ . The generating function also depends on source variables  $j = \text{diag}(j_1, \dots, j_k)$ . The scaling of the variables  $\xi_a$  with  $lp$  anticipates the local scale for spectral fluctuations inside the macroscopic bulk in which the unscaled variables  $x_a$  are assumed to lie. The latter variables  $x_a$  may also be degenerate, *i.e.*  $x_a = x_b$  for some  $a, b = 1, \dots, p$ , as long as the eigenvalues  $x_a + \xi_a/(lp)$  are pairwise different. The scaling of  $\xi_a$  has to be adjusted when one or more of the variables  $x_a$  are at an edge of the spectrum. The generating function reads

$$Z_{k,k}^{(p,n)}(\kappa) = \int d[W] P(W|C) \prod_{b=1}^k \frac{\det(WW^T - \kappa_{b,2}\mathbb{1}_{lp})}{\det(WW^T - \kappa_{b,1}\mathbb{1}_{lp})}, \quad (4)$$

with  $d[\cdot]$  being the flat measure, *i.e.* the product of all independent differentials. The matrix  $\mathbb{1}_{lp}$  is the  $lp$  dimensional identity matrix.

To conveniently study the asymptotics for large  $n, p$  with  $p/n = \gamma^2$  fixed, we employ the supersymmetry method, see Refs. [28, 29, 36, 39, 40]. A more mathematical introduction into superanalysis can be found in Ref. [42]. Using the results in Refs. [20, 22, 43], we map the generating function (4) to superspace,

$$Z_{k,k}^{(p,n)}(\kappa) = K_{nl,k} \text{sdet}^{(n-p)l/2} \tilde{\kappa} \int d[\sigma] \text{sdet}^{(nl-1)/2} \sigma \exp\left(\frac{nl}{2} \text{str} \tilde{\kappa} \sigma\right) \text{sdet}^{-l/2} (\mathbb{1}_p \otimes \mathbb{1}_{2k|2k} + \imath \Lambda \otimes \sigma), \quad (5)$$

where  $\tilde{\kappa} = \text{diag}(\kappa_{1,1}, \dots, \kappa_{k,1}, \kappa_{1,2}, \dots, \kappa_{k,2}) \otimes \mathbb{1}_2$  is viewed as a  $(2k|2k) \times (2k|2k)$  diagonal supermatrix. The factor of 2 in the dimensions occurs because we study the *real* correlated Wishart ensemble. The  $(2k|2k) \times (2k|2k)$  supermatrix  $\tilde{L}\sigma$  has a positive definite symmetric matrix in the boson–boson block  $\sigma_{\text{BB}}$  while the fermion–fermion block  $\sigma_{\text{FF}}$  belongs to the circular symplectic ensemble [43–46]. The boson–fermion block  $\sigma_{\text{BF}} = \{\eta_{ab}, \eta_{ab}^*\}_{a=1, \dots, 2k; b=1, \dots, k}$  consists of  $2k$  real independent Grassmann variables and the fermion–boson block is  $\sigma_{\text{FB}} = -\sigma_{\text{BF}}^\dagger$  with the dagger denoting the ordinary adjoint. Here we have employed the supermatrix  $\tilde{L} = \text{diag}(L_1, \dots, L_k) \otimes \mathbb{1}_{1|1} \otimes \mathbb{1}_2$  encoding the signs of the imaginary increment  $\varepsilon$ . The normalization constant

$$K_{nl,k}^{-1} = \int d[\sigma] \text{sdet}^{(nl-1)/2} \sigma \exp\left(-\frac{nl}{2} \text{str} \tilde{L} \sigma\right), \quad (6)$$

is determined by the condition that  $Z_{k,k}^{(p,n)} \rightarrow 1$  for  $\varepsilon \rightarrow \infty$ . By construction, we also have  $Z_{k,k}^{(p,n)}(\kappa)|_{j=0} = 1$  for vanishing source variables. To show the non-trivial equality of the integral (6) for the normalization constant and the integral (5) for  $j = 0$ , one needs Cauchy-like integral theorems [34, 36, 47–49] first derived by Wegner [35] for arbitrary supermatrix sizes. The measure  $d[\sigma]$  is the product of all differentials of the independent variables. The integration over Grassmann variables are normalized as

$$\int d\eta = 0, \quad \int \eta d\eta = 1, \quad (7)$$

which differs from another convention by a factor of  $\sqrt{2\pi}$ . With this choice the constant  $K_{nl,k}$  becomes in the large  $n$  limit

$$K_{\infty,k} = \lim_{n \rightarrow \infty} K_{nl,k} = 4^{-k} (2\pi^2)^{-k^2} \quad (8)$$

because the integrand can be expanded around  $\sigma_0 = \tilde{L}$  yielding a Gaussian integral.

In the supermatrix representation (5) we differentiate with respect to the source variables  $j_a$  and set them to zero. Then we perform a  $1/p$  expansion by means of a saddle point approximation. We expand around the saddle point

matrix  $\sigma_0$  according to  $\sigma = \sigma_0 + \delta\sigma/\sqrt{p}$  where the scaling  $\sqrt{p}$  of the massive modes  $\delta\sigma$  is dictated by the fact that all variables  $x_a$  are in the bulk of the spectrum. After keeping only the leading order term we find

$$R_k(x, \xi) = K_{nl,k} \lim_{\varepsilon \rightarrow 0} \int d[\sigma_0, \delta\sigma] \sum_{L_1, \dots, L_k = \pm 1} \exp\left(-\frac{nl}{2} \mathcal{L}\left(\sigma_0 + \frac{\delta\sigma}{\sqrt{p}}\right)\right) \times \prod_{j=1}^k \left(\frac{L_j}{8\pi\gamma^2} \text{str}\left(\sigma_0 + \frac{\delta\sigma}{\sqrt{p}}\right) \begin{bmatrix} e_{jj}^k & 0 \\ 0 & -e_{jj}^k \end{bmatrix} \otimes \mathbb{1}_2 + \frac{\gamma^{-2} - 1}{2\pi i} \frac{L_j}{x_j + iL_j\varepsilon}\right) + \mathcal{O}\left(\frac{1}{p}\right) \quad (9)$$

with  $\gamma^2 = p/n$ . Here  $e_{ab}^k$  is a  $k \times k$  matrix with zeros everywhere and unity in the  $(a, b)$  entry. For the time being, neither the saddle point manifold of  $\sigma_0$ , referred to as Goldstone modes, nor the support of the massive modes  $\delta\sigma$  are precisely specified. The second term  $1/(x_j + iL_j\varepsilon)$  in the above product is reminiscent of the superdeterminant in front of the integral (5). It generates Dirac  $\delta$  functions  $\delta(x_j)$  which have the following origin: To derive the expression (5) we used  $WW^T$  instead of  $W^TW$ . Their spectra only differ in the number of the generic zero eigenvalues which is equal to  $n - p = (\gamma^{-2} - 1)p$  for  $W^TW$  and zero for  $WW^T$ . We return to these terms in subsection III B. Keeping with the common terminology, we refer to the function

$$\mathcal{L}(\sigma) = \frac{\gamma^2}{p} \sum_{i=1}^p \text{str} \ln(\mathbb{1}_{2k|2k} + i\Lambda_i\sigma) - i \text{str} \left( \tilde{x} + i\varepsilon\tilde{L} + \frac{\tilde{\xi}}{pl} \right) \sigma - \left(1 - \frac{\gamma^2}{pl}\right) \text{str} \ln \sigma. \quad (10)$$

in the above expression as ‘‘Lagrangian’’.

### B. Testing the limit of large matrix dimensions

We now show that the limit  $p, n \rightarrow \infty$  with  $0 < \gamma^2 = p/n \leq 1$  fixed is well-defined, because  $|\text{sdet}^{-1}(1 + i\Lambda_i\sigma)|$  is bounded. For the numerical part  $\hat{\sigma}$  of  $\sigma$  we have

$$\left| \text{sdet}^{-1} \left( \mathbb{1}_{2k|2k} + i \frac{\Lambda_i}{2\Lambda_{\max}} \hat{\sigma} \right) \right| = \frac{\prod_{j=1}^k |1 + i\Lambda_j e^{i\varphi_j} / (2\Lambda_{\max})|^2}{\prod_{j=1}^{2k} |1 + iL_j \Lambda_i e^{\theta_j} / (2\Lambda_{\max})|}, \quad (11)$$

where  $e^\theta = \tilde{L} \text{diag}(e^{\theta_1}, \dots, e^{\theta_{2k}}) / (2\Lambda_{\max})$  are the eigenvalues of the boson–boson block  $\sigma_{\text{BB}}$  of  $\sigma$  and  $e^{i\varphi} = \text{diag}(e^{i\varphi_1}, \dots, e^{i\varphi_k}) \otimes \mathbb{1}_2 / (2\Lambda_{\max})$  are the eigenvalues of the fermion–fermion block  $\sigma_{\text{FF}}$ . Here we rescaled  $\sigma \rightarrow \sigma / (2\Lambda_{\max})$  with  $\Lambda_{\max}$  being the largest of the empirical eigenvalues  $\Lambda$ . The expression (11) is bounded from below and above according to

$$0 < \frac{(1 - \Lambda_i / (2\Lambda_{\max}))^{2k}}{\prod_{j=1}^{2k} (1 + e^{2\theta_j} \Lambda_i / (2\Lambda_{\max}))} \leq \left| \text{sdet}^{-1} \left( \mathbb{1}_{2k|2k} + i \frac{\Lambda_i}{2\Lambda_{\max}} \hat{\sigma} \right) \right| \leq \left(1 + \frac{\Lambda_i}{2\Lambda_{\max}}\right)^{2k} < \infty. \quad (12)$$

These bounds are integrable due to the terms  $\exp[-nl\varepsilon e^{\theta_j}/2]$  and  $e^{(nl-1)\theta_j/2}$  and due to  $k \leq p \leq n$  in the integrand. This estimate only holds for the part of  $\prod_{i=1}^p |\text{sdet}^{-1}(\mathbb{1}_{2k|2k} + i\Lambda_i\sigma)|$  without the Grassmann variables. An expansion in the Grassmann variables yields a finite polynomial in powers of the matrices

$$\frac{1}{p} \sum_{i=1}^p \frac{1}{(2\Lambda_{\max}/\Lambda_i \mathbb{1}_{2k} + i\sigma_{\text{BB}})^{\otimes m}} \otimes \frac{1}{(2\Lambda_{\max}/\Lambda_i \mathbb{1}_{2k} + i\sigma_{\text{FF}})^{\otimes m}} \quad (13)$$

which are contracted in the generating function (5), the details do not matter. The tensor product multiplies the space corresponding to the  $2k \times 2k$  boson–boson block with the one corresponding to the  $2k \times 2k$  fermion–fermion block. The exponent  $m = 0, \dots, 2k^2$  is taken in a tensor sense, too. The modulus of the spectrum of these matrices are bounded from above by  $2^{-2m}$  independent of  $\Lambda$  and  $\hat{\sigma}$ . Therefore the limit  $p, n \rightarrow \infty$  with  $0 < \gamma^2 = p/n \leq 1$  fixed is well-defined if we assume that

$$\lim_{p \rightarrow \infty} \frac{1}{p} \sum_{i=1}^p \ln(1 + s\Lambda_i) < \infty \quad (14)$$

remains finite for any  $s > -1/\Lambda_{\max}$  and in the case that  $\Lambda_{\max}/\Lambda_i$  also remains finite. This is realized when the smallest eigenvalues is of the same order as the largest eigenvalue  $\Lambda_{\max}$ .

If  $\Lambda$  contains a finite number  $p_{\text{out}}$  of outliers of larger order as the ones in the bulk, we may still resort to the discussion above. We split the product of superdeterminants in two parts,

$$\prod_{i=1}^p \text{sdet}^{-l/2} (\mathbb{1}_{2k|2k} + \imath \Lambda_i \sigma) = \prod_{i=1}^{p-p_{\text{out}}} \text{sdet}^{-l/2} (\mathbb{1}_{2k|2k} + \imath \Lambda_i \sigma) \prod_{i=p-p_{\text{out}}+1}^p \text{sdet}^{-l/2} (\mathbb{1}_{2k|2k} + \imath \Lambda_i \sigma). \quad (15)$$

Only the first product enters the saddle point equation to be given in the sequel while the second one may be considered as a  $p$ -independent perturbation of the integrand. The second product cannot contribute to the saddle point analysis since the number of outliers  $p_{\text{out}}$  is assumed to be fixed. The physical interpretation is that outliers which are macroscopically separated from or may even lie on a scale larger than that of the bulk do not influence the statistics in the bulk. We study the outliers in more detail in subsection IV A.

Another remark is in order, clarifying how the existence of a limiting distribution  $\rho(\lambda)$  for the empirical eigenvalues  $\Lambda$  affects the above discussion. Such a distribution exists if

$$\lim_{p \rightarrow \infty} \frac{1}{p} \sum_{i=1}^p f(\Lambda_i) = \int_0^{\infty} f(\lambda) \rho(\lambda) d\lambda, \quad (16)$$

whenever the test function  $f$  is integrable with respect to  $\rho$  and  $f(\Lambda_i) < \infty$ . The sum in the Lagrangian (10) is then bounded from above and below by the average of the integral of the supermatrix resolvent,

$$\lim_{p \rightarrow \infty} \frac{1}{p} \sum_{i=1}^p \text{str} \ln (\mathbb{1}_{2k|2k} + \imath \Lambda_i \sigma) = \int_0^{\infty} \text{str} \ln (\mathbb{1}_{2k|2k} + \imath \lambda \sigma) \rho(\lambda) d\lambda. \quad (17)$$

Outliers appear as Dirac  $\delta$  functions in  $\rho$ . Although Eqs. (16) and (17) are only valid if a limiting distribution for the empirical eigenvalues  $\Lambda$  exists, we want to find an expression which still provides a good approximation at finite matrix dimensions  $p$  and  $n$ .

### III. BULK STATISTICS

We analyze the bulk statistics in three steps. First we discuss the saddle point approximation for a general  $k$ -point correlation function in section III A. In section III B an explicit and very simple relation between the macroscopic level density and the saddle point solution is presented. In section III C we show that inside the bulk the whole spectral statistics on the local scale agrees with the sine kernel of real matrices. This is true and exact for all  $k$ -point correlation functions including the cumbersome Efetov–Wegner boundary terms, see Refs. [50, 51].

#### A. Saddle point approximation in the bulk

We now show that, assuming the condition (14), the  $k$ -point correlation function is independent of the degree  $l$  of degeneracy in leading order of a  $1/p$  expansion. To this end, we carry out a saddle point approximation of the integral (9) by expanding the Lagrangian (10) up to the order  $1/p$ ,

$$\begin{aligned} \mathcal{L} \left( \sigma_0 + \frac{\delta \sigma}{\sqrt{p}} \right) &= \frac{\gamma^2}{p} \sum_{i=1}^p \text{str} \ln (\mathbb{1}_{2k|2k} + \imath \Lambda_i \sigma_0) - \imath \text{str} \left( \tilde{x} + \imath \varepsilon \tilde{L} \right) \sigma_0 - \left( 1 - \frac{\gamma^2}{pl} \right) \text{str} \ln \sigma_0 \\ &+ \frac{\imath}{\sqrt{p}} \text{str} \left[ \frac{\gamma^2}{p} \sum_{i=1}^p \frac{\Lambda_i}{\mathbb{1}_{2k|2k} + \imath \Lambda_i \sigma_0} - \tilde{x} - \imath \varepsilon \tilde{L} + \imath \sigma_0^{-1} \right] \delta \sigma \\ &+ \frac{1}{2p} \text{str} \left[ \frac{\gamma^2}{p} \sum_{i=1}^p \left( \frac{\Lambda_i}{\mathbb{1}_{2k|2k} + \imath \Lambda_i \sigma_0} \delta \sigma \right)^2 + (\sigma_0^{-1} \delta \sigma)^2 - \imath \frac{2}{l} \tilde{\xi} \sigma_0 \right] + \mathcal{O} \left( \frac{1}{p^{3/2}} \right). \end{aligned} \quad (18)$$

The term of first order in  $\delta \sigma$  yields the supermatrix valued saddle point equation

$$\tilde{x} Q + \mathbb{1}_{2k|2k} - \frac{\gamma^2}{p} \sum_{i=1}^p \frac{\Lambda_i Q}{\mathbb{1}_{2k|2k} + \Lambda_i Q} = 0, \quad (19)$$

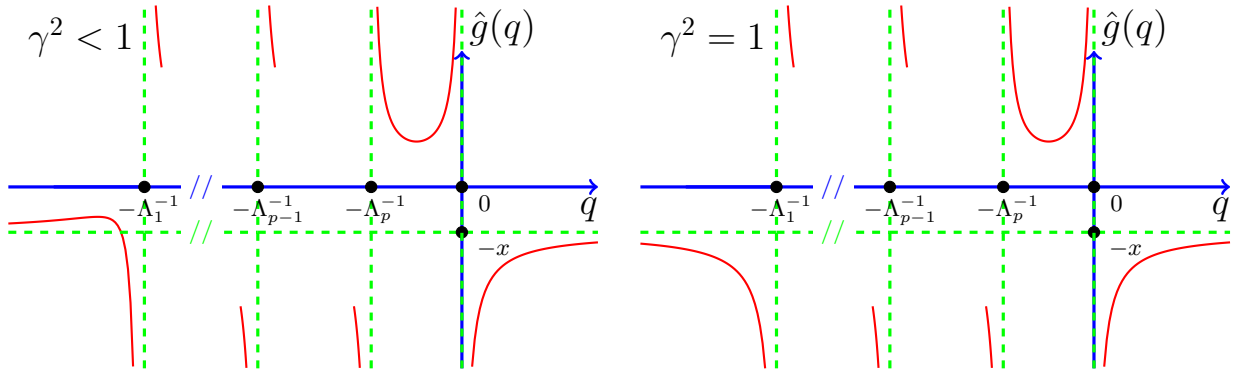


FIG. 1: (Color online) Asymptotic schematic behaviour of the rational function  $\hat{g}(q, x)$  (solid curves) at the singularities (dashed) and at infinity, *cf.* Eq. (20). The variable  $x$  stands for any eigenvalue  $x_1, \dots, x_k$  of the correlated Wishart matrix  $WW^T$ . The qualitative convexity properties for  $q > -1/\Lambda_p$  are also shown. However the behaviour for  $q < -1/\Lambda_p$  strongly depends on the parameter  $\gamma^2 = p/n$  and the empirical eigenvalues  $\Lambda_a$ . Concretely, we only have a maximum above the horizontal green line for  $q < -1/\Lambda_1$  when  $\gamma^2 < 1$  (left figure) and no maximum at all for  $\gamma^2 = 1$  (right figure). In the latter case  $g$  approaches the value  $-1$  for  $q \rightarrow -\infty$  from below instead from above. Moreover we may have maximally one maximum and one minimum inside any of the intervals  $] -1/\Lambda_j, -1/\Lambda_{j+1}[$  or none at all, depending on the distance between the individual  $\Lambda_a$ .

where  $Q$  denotes the solution. We neglect the term in  $\varepsilon$  as it is infinitesimal. The difficulty is that the saddle point solution  $Q = \imath\sigma$  depends in a highly non-trivial way on the empirical eigenvalues  $\Lambda_i$ .

The saddle point equation is essentially scalar, as may be seen by taking the commutator of Eq. (19) with  $Q^{-1}$ . We obtain  $\tilde{x} = Q^{-1}\tilde{x}Q$  implying that  $Q$  and  $\tilde{x}$  commute. Thus, we can analyze Eq. (19) in the space of the eigenvalues of  $Q$ . There are two kinds of eigenvalues, namely  $q^{(b)} = \text{diag}(q_1^{(b)}, \dots, q_{2k}^{(b)})$  in the boson-boson block and  $q^{(f)} = \text{diag}(q_1^{(f)}, \dots, q_k^{(f)}) \otimes \mathbb{1}_2$  in the fermion-fermion block. The double degeneracy of the latter is the Kramers degeneracy for quaternion matrices. The integration domain is non-compact for  $q^{(b)}, q_j^{(b)} \in \imath L_j \mathbb{R}_+$  with  $L_j = \pm 1$ , and compact for  $q^{(f)}, q_j^{(f)} \in \text{U}(1)$ . Hence we only need to analyze the scalar saddle point equation

$$0 = -x_a - \frac{1}{q(x_a)} + \frac{\gamma^2}{p} \sum_{i=1}^p \frac{\Lambda_i}{1 + \Lambda_i q(x_a)} = -x_a + g(q(x_a)) = \hat{g}(q(x_a), x_a), \quad (20)$$

where we introduce the functions  $q(x_a)$ ,  $g(q(x_a)) = \hat{g}(q(x_a), 0)$  and  $\hat{g}(q(x_a), x_a)$ . Anticipating the following discussion, we mention that the level density is directly related to the solutions of this equation. It is a classical result in high dimensional inference [30–33] where it was derived by other means. Marčenko and Pastur [30] showed that, if this equation has a solution in the upper half-plane, this solution is unique, which we denote by  $q_0(x_a)$ . Although Marčenko and Pastur already discussed the following setting in more generality, namely for an arbitrary density  $\rho$  in Eq. (16), we want to analyze the rational function  $g(q)$  at finite matrix dimension  $p$ , in particular its singularities. We need results of this discussion for the analysis of the spectral statistics on the level of the local level spacing.

The equation  $\hat{g}(q(x_a), x_a) = 0$  has  $p + 1$  roots for each  $x_a$ . Moreover the function  $g(q)$  is singular at  $q = -1/\Lambda_i$  for  $i = 1, \dots, p$  and at  $q = 0$ . An asymptotic analysis of the singularities yields

$$\lim_{q \rightarrow 0^\pm} g(q) = \mp \infty, \quad \lim_{q \rightarrow (-1/\Lambda_i)^\pm} g(q) = \pm \infty, \quad (21)$$

where  $\pm$  indicates the limit from above or below, respectively. For  $q \rightarrow \pm\infty$  we obtain

$$\hat{g}(q(x_a), x_a) \rightarrow -x_a - \frac{1 - \gamma^2}{q} - \sum_{i=1}^p \frac{\gamma^2}{p\Lambda_i} \frac{1}{q^2} \quad (22)$$

with  $\gamma^2 = p/n \leq 1$ . Figure 1 shows the asymptotic behaviour of  $\hat{g}(q, x)$ . As there is at least one real root of  $g(q)$  within each interval  $(-1/\Lambda_{i+1}, -1/\Lambda_i)$  for  $i = 1, \dots, p - 1$ , at least  $p - 1$  out of  $p + 1$  roots are real. Since Eq. (20) is real, the complex conjugate  $q_0^*(x_a)$  of a solution  $q_0(x_a)$  solves Eq. (20) as well. Hence, the remaining two roots are either a complex conjugate pair or both real.

When a complex conjugate pair solves the saddle point equation, the eigenvalues  $q_j^{(b)}$  in the boson-boson block of the supermatrix  $Q$  can only reach those solutions which share the same sign of the imaginary part with  $x_a + \imath L_a \varepsilon$ .

This is due to the infinitely high potential walls around the singularities  $q = -1/\Lambda_i$  when  $p \rightarrow \infty$ . In contrast, the eigenvalues  $q_j^{(f)}$  in the fermion–fermion block reach both saddle points. When diagonalizing the supermatrix  $Q$  we obtain the Berezinian, *i.e.*, the superspace Jacobian,

$$B_{2k|k}(q^{(b)}; q^{(f)}) = \frac{|\Delta_{2k}(q^{(b)})|^3 \Delta_k^6(q^{(f)})}{\Delta_{3k}^2(q^{(b)}; q^{(f)})} \quad (23)$$

with the Vandermonde determinant  $\Delta_k(q^{(f)}) = \prod_{1 \leq i < j \leq k} (q_j^{(f)} - q_i^{(f)})$ . Plugging the two kinds of saddle points into this Berezinian, we observe the following. Solutions in which the eigenvalues of the boson–boson block and the fermion–fermion block do not agree are algebraically suppressed by factors of  $1/p$  and thus smaller than those in which the spectra of the boson–boson and the fermion–fermion blocks counted with multiplicities coincide.

In the case that all solutions are real we may reach more than one saddle point with the boson–boson block of  $Q$ . However only one of all real saddle points contributes, as can be seen by considering the first and second derivative of  $g$  (second and third derivative of the Lagrangian (10)) which read

$$g'(q) = \frac{1}{q^2} - \frac{\gamma^2}{p} \sum_{i=1}^p \frac{\Lambda_i^2}{(1 + \Lambda_i q)^2}, \quad g''(q) = -\frac{3}{q^3} + \frac{3\gamma^2}{p} \sum_{i=1}^p \frac{\Lambda_i^3}{(1 + \Lambda_i q)^3}. \quad (24)$$

For  $q \in ]-1/\Lambda_p, 0[$  the estimate

$$g''(q) \geq 3\gamma^2 \lambda_p^3 - \frac{3}{q^3} \geq 3(\gamma^2 + 1)\Lambda_p^3 > 0 \quad (25)$$

holds, because of  $(q + 1/\Lambda_j)^{-3} \geq \Lambda_j^3$  for all  $j = 1, \dots, p$ . Hence,  $g$  is concave in this interval, *cf.* Fig. 1. We find a similar estimate for  $q > 0$ , namely

$$g''(q) \leq 3\frac{\gamma^2 - 1}{q^3} \leq 0 \quad (26)$$

implying that  $g$  is convex on the positive real line. We recall that  $\gamma^2 \leq 1$  because of  $p \leq n$ .

When  $q$  is between two empirical eigenvalues, in particular  $q \in ]-1/\Lambda_j, -1/\Lambda_{j+1}[$  with  $j = 1, \dots, p-1$ , we find either not an extremum or a single pair of a minimum and a maximum. This is so because of the following reason. The curvature of  $g'$  is the third derivative of  $g$ ,

$$\begin{aligned} \frac{g^{(3)}(q)}{6} &= \frac{1}{q^4} - \frac{\gamma^2}{p} \sum_{i=1}^p \frac{\Lambda_i^4}{(1 + \Lambda_i q)^4} \\ &< \left( \frac{\gamma^2}{p} \sum_{i=1}^p \frac{\Lambda_i^2}{(1 + \Lambda_i q)^2} \right)^2 - \frac{\gamma^2}{p} \sum_{i=1}^p \frac{\Lambda_i^4}{(1 + \Lambda_i q)^4} \\ &\leq \max \left\{ 0, \left( \frac{1}{p} \sum_{i=1}^p \frac{\Lambda_i^2}{(1 + \Lambda_i q)^2} \right)^2 - \frac{1}{p} \sum_{i=1}^p \frac{\Lambda_i^4}{(1 + \Lambda_i q)^4} \right\} \\ &\leq 0 \end{aligned} \quad (27)$$

for all  $q$  satisfying  $g'(q) < 0$ . Hence  $g'(q)$  is convex in these regimes and it may have either no or two zero points (counted with multiplicities) in the intervals  $]-1/\Lambda_j, -1/\Lambda_{j+1}[$  implying the extrema for  $g(q)$ . In the second, third and fourth line of Eq. (27) we employed the assumption  $g'(q) < 0$ , the fact that the right hand side is a concave function in  $\gamma^2 \in [0, 1]$  and that the second term in the maximization is the negative variance of the sequence  $\Lambda_i^2/(1 + \Lambda_i q)^2$ ,  $i = 1, \dots, p$ . The estimate (27) also tells us that for  $q < -1/\Lambda_1$  the function has either a single maximum or none at all depending on whether  $\gamma^2 < 1$  or  $\gamma^2 = 1$ , respectively.

Altogether, we know that the function  $g$  has at each real value  $x$  either  $p-1$  or  $p+1$  real zeros counted with multiplicities. Only those solutions  $q_0(x)$  where  $g(q_0(x))$  has a positive slope correspond to a minimum of the Lagrangian (10) in the eigenvalues of the boson–boson block of  $-Q\tilde{x}^{-1} = -\tilde{L}\sigma\tilde{x}^{-1}$ . The asymptotic behaviour and the convexity properties of the rational function  $g$  imply that in the case of  $p+1$  real solutions only one of those solutions has a positive slope at  $g(q_0(x))$ . Consequently, the non-compact integrals are evaluated at this saddle point only regardless what sign  $L_a$  is chosen. A similar argument holds for the compact integrals over  $q_f$  in the fermion-fermion block which sees exactly the same point as a minimum as the eigenvalues  $q_f$  and all other real solutions appear as

maxima in the Lagrangian (10). Despite the fact that the contours of  $q^{(b)}$  and  $q^{(f)}$  orthogonally cross each other at the saddle point  $q_0(x)$ , the opposite sign in the supertrace renders the saddle point for both contours a minimum. Summing over  $L$  in Eq. (3) we notice that those terms where the contributing saddle point solution is real vanish because the contributing saddle point is independent of the corresponding sign. Therefore only the complex solutions contribute. We thus omit all real roots in the following.

Since  $Q$  and  $\tilde{x}$  commute, we may choose an appropriate block diagonal basis,  $Q = \text{diag}(Q^{(1)}, \dots, Q^{(\alpha)})$  where  $\alpha < k$  is the number of distinct points  $x_a$ , and discuss the resulting saddle point equation for each block separately. The size of a single block depends on the degeneracy  $m_o$  of the point  $x^{(o)}$  in question,  $o = 1, \dots, \alpha$ , *i.e.* if  $x_{i_1} = x_{i_2} = \dots = x_{i_{m_o}}$  the corresponding block is of dimension  $(2m_o|2m_o)$  in superspace. By  $\tilde{L}^{(o)} = L^{(o)} \otimes \mathbb{1}_{|1|1} \otimes \mathbb{1}_2$  we denote the projection of  $\tilde{L}$  onto the block corresponding to the point  $x^{(o)}$ . The resulting saddle point equation is invariant with respect to  $\text{UOSp}(\tilde{L}^{(1)}) \times \dots \times \text{UOSp}(\tilde{L}^{(\alpha)})$ , where  $\text{UOSp}(\tilde{L}^{(o)})$  is the group of pseudo-unitary orthosymplectic matrices  $T$  with the property  $T \text{diag}(L^{(o)} \otimes \mathbb{1}_2; \mathbb{1}_{2m_o}) T^\dagger = \text{diag}(L^{(o)} \otimes \mathbb{1}_2; \mathbb{1}_{2m_o})$ . Hence, instead of isolated saddle points we obtain saddle point manifolds, see Refs. [28, 29, 36, 39, 44] in another context. From the discussion above, we have to integrate  $Q = \imath\sigma_0 = \text{diag}(Q^{(1)}, \dots, Q^{(\alpha)})$  with

$$\begin{aligned} Q^{(o)} &= \text{Re } q_0(x^{(o)}) \mathbb{1}_{m_o} + \imath T^{(o)} \text{Im } q_0 \left( x^{(o)} + \imath \tilde{L}^{(o)} \varepsilon \right) T^{(o)-1} \\ &\approx \text{Re } q_0(x^{(o)}) \mathbb{1}_{m_o} + \imath \text{Im } q_0(x^{(o)}) T^{(o)} \tilde{L}^{(o)} T^{(o)-1} \end{aligned} \quad (28)$$

over the coset

$$T^{(o)} \in \text{UOSp}(\tilde{L}^{(o)}) / [\text{UOSp}(2m_0^{(o)}|2m_0^{(o)}) \times \text{UOSp}(2m_1^{(o)}|2m_1^{(o)})] \quad (29)$$

which parametrizes the ‘‘Goldstone modes’’. The variables  $2m_0^{(o)}$  and  $2m_1^{(o)}$  are the numbers of +1’s and –1’s in  $\tilde{L}^{(o)}$  such that  $m_0^{(o)} + m_1^{(o)} = m_o$ .

We now turn to the integration over the ‘‘massive modes’’, parametrized by

$$\delta\sigma = T \begin{bmatrix} \delta\sigma_{11} & \cdots & \delta\sigma_{1\alpha} \\ \vdots & & \vdots \\ \delta\sigma_{\alpha 1} & \cdots & \delta\sigma_{\alpha\alpha} \end{bmatrix} T^{-1} \quad (30)$$

where  $T = \text{diag}(T^{(1)}, \dots, T^{(\alpha)})$  and where  $\delta\sigma_{ab}$  is a  $(2m_a|2m_a) \times (2m_b|2m_b)$  supermatrix. The diagonal blocks satisfy the commutation relations  $[\delta\sigma_{oo}, \tilde{L}^{(o)}] = 0$  since the remaining integration, in particular the components which do not commute, is accounted for by the integrals over  $T^{(o)}$ . The challenging part in specifying the whole symmetries of the blocks  $\delta\sigma_{ab}$  are the phases in front. The quadratic part in  $\delta\sigma$  of the Lagrangian (18) has to be positive definite and must ensure convergence. We define the complex numbers

$$z_{ab}^{(+)} = \frac{\gamma^2}{p} \sum_{i=1}^p \frac{1}{\Lambda_i^{-1} + q_0(x^{(a)})} \frac{1}{\Lambda_i^{-1} + q_0(x^{(b)})} - \frac{1}{q_0(x^{(a)})q_0(x^{(b)})} \quad (31)$$

and

$$z_{ab}^{(-)} = \frac{\gamma^2}{p} \sum_{i=1}^p \frac{1}{\Lambda_i^{-1} + q_0(x^{(a)})} \frac{1}{\Lambda_i^{-1} + (q_0(x^{(b)}))^*} - \frac{1}{q_0(x^{(a)})(q_0(x^{(b)}))^*}, \quad (32)$$

allowing us to split the matrix blocks as follows

$$\delta\sigma_{aa} = \frac{1}{\sqrt{z_{aa}^{(+)}}} \delta\sigma_{aa}^{(00)} + \frac{1}{\sqrt{(z_{aa}^{(+)})^*}} \delta\sigma_{aa}^{(11)}, \quad (33)$$

$$\delta\sigma_{ab} \stackrel{a \leq b}{=} \frac{1}{\sqrt{z_{ab}^{(+)}}} \delta\sigma_{ab}^{(00)} + \frac{1}{\sqrt{(z_{ab}^{(+)})^*}} \delta\sigma_{ab}^{(11)} + \frac{1}{\sqrt{z_{ab}^{(-)}}} \delta\sigma_{ab}^{(01)} + \frac{1}{\sqrt{(z_{ab}^{(-)})^*}} \delta\sigma_{ab}^{(10)}, \quad (34)$$

$$\delta\sigma_{ab} \stackrel{a \geq b}{=} \frac{1}{\sqrt{z_{ab}^{(+)}}} \delta\sigma_{ab}^{(00)\dagger} + \frac{1}{\sqrt{(z_{ab}^{(+)})^*}} \delta\sigma_{ab}^{(11)\dagger} + \frac{1}{\sqrt{z_{ab}^{(-)}}} \delta\sigma_{ab}^{(01)\dagger} + \frac{1}{\sqrt{(z_{ab}^{(-)})^*}} \delta\sigma_{ab}^{(10)\dagger}, \quad (35)$$

such that  $\tilde{L}^{(i)} \delta\sigma_{ab}^{(ij)} \tilde{L}^{(j)} = (-1)^{i+j} \delta\sigma_{ab}^{(ij)}$ . Blocks of the form  $\delta\sigma_{aa}^{(01)}$  and  $\delta\sigma_{aa}^{(10)}$  do not exist, because of the required commutation relation with  $\tilde{L}^{(a)}$ . We recall the dimensions  $m_0^{(a)}$  and  $m_1^{(a)}$  which essentially are the signature of  $\tilde{L}^{(a)}$ .

The diagonal matrix blocks  $\delta\sigma_{aa}^{(jj)}$  are Hermitian supermatrices of dimension  $(2m_j^{(a)}|2m_j^{(a)}) \times (2m_j^{(a)}|2m_j^{(a)})$  where the boson–boson blocks are real symmetric and the fermion–fermion blocks are Hermitian self–dual. The off–diagonal block  $\delta\sigma_{ab}^{(ij)}$  has dimension  $(2m_i^{(a)}|2m_i^{(a)}) \times (2m_j^{(b)}|2m_j^{(b)})$ . Its boson–boson block is an arbitrary real matrix and its fermion–fermion block an arbitrary quaternion matrix. The integration measure of  $T$  is the Haar measure on the coset and the one of  $\delta\sigma$  is the flat Lebesgue measure for the commuting and the Berezin measure for the anticommuting variables. The Lagrangian (18) takes the form

$$\begin{aligned} \mathcal{L}\left(\sigma_0 + \frac{\delta\sigma}{\sqrt{p}}\right) &= -i \sum_{o=1}^{\alpha} \text{Im } q_0(x^{(o)}) \text{str} \left( i\varepsilon \tilde{L}^{(o)} + \frac{\tilde{\xi}^{(o)}}{pl} \right) T^{(o)} \tilde{L}^{(o)} T^{(o)-1} \\ &+ \frac{1}{p} \sum_{1 \leq a < b \leq \alpha} \sum_{i,j=0,1} \text{str} \delta\sigma_{ab}^{(ij)} \delta\sigma_{ab}^{(ij)\dagger} + \frac{1}{2p} \sum_{a=1}^{\alpha} \sum_{j=0,1} \text{str} (\delta\sigma_{aa}^{(jj)})^2 + \mathcal{O}\left(\frac{1}{p^{3/2}}\right) \end{aligned} \quad (36)$$

where  $\tilde{\xi} = \text{diag}(\tilde{\xi}^{(1)}, \dots, \tilde{\xi}^{(\alpha)})$  is splitted analogously to  $\tilde{L}$ . The prefactors of the individual blocks  $\delta\sigma_{ab}^{(ij)}$ , see Eqs. (33–35), cancel in the Berezinian of the change of coordinates for the supermatrix  $\sigma$  into the Goldstone and the massive modes because we have for each of these blocks the same number of real variables and Grassmann variables.

To proceed we have to carefully analyze the Efetov–Wegner boundary terms [35, 36]. They are an inherent feature of superanalysis without counterpart in ordinary analysis. These terms appear whenever a change of variables is performed on superspaces with boundaries, including those boundaries induced by coordinate singularities of the Berezinian.

## B. Macroscopic Level Density

In the case of the macroscopic level density, *i.e.*,  $k = 1$ ,  $\xi_1 = 0$  and  $\tilde{L}^{(1)} = L_1^{(1)} \mathbb{1}_{2|2}$ , Efetov–Wegner boundary terms cannot appear because we only shift and rescale the supermatrix  $\sigma \rightarrow \delta\sigma$ . The Gaussian integral over  $\delta\sigma$  cancels the constant  $\lim_{n \rightarrow \infty} K_{nl,1} = 1/(8\pi^2)$  in the limit  $n \rightarrow \infty$ . The level density becomes

$$R_1(x) \stackrel{n \gg 1}{\approx} \lim_{\varepsilon \rightarrow 0} \text{Im} \left( \frac{1}{\gamma^2 \pi} q_0(x + i\varepsilon) + \frac{\gamma^{-2} - 1}{\pi} \frac{1}{x + i\varepsilon} \right) = \frac{1}{\gamma^2 \pi} \text{Im } q_0(x), \quad (37)$$

for all values of  $l$ . Hence, the saddle point solution  $q_0(x)$  is up to the normalization  $1/\gamma^2$  the Green function — also known as Cauchy or Stieltjes transform — of the density  $R_1(x)$ . When writing  $\text{Im } q_0(x)$  shorthand, we view the  $1/x$  singularity of  $q_0(x)$  at the origin as a real term which may be neglected. Thus, the chain of equalities (37) is consistent.

The coincidence of  $q_0(x)/\gamma^2$  with the Green function implies that the function  $g(q) - 1/q$ , see Eq. (20), can be identified with the R transform in the theory of free probability. An introduction to free probability in random matrix theory can be found in Ref. [52, 53].

The Dirac  $\delta$  function or equivalently the second term under the limit in Eq. (37) is important for  $\gamma^2 < 1$  when the limit  $\varepsilon \rightarrow 0$  is still to be taken. To clarify this we consider the asymptotics of the saddle point solution for  $x + i\varepsilon \rightarrow 0$  which is equivalent to  $q \rightarrow -\infty$ , *cf.* Fig. 1. We employ the asymptotics (22) of the function  $\hat{g}$ . Taking into account the first two terms only we find the asymptotic behaviour of the saddle point solution as  $q_0(x + i\varepsilon) \approx (\gamma^2 - 1)/(x + i\varepsilon)$  for  $|x + i\varepsilon| \ll 1$ . The imaginary part of this term yields in the limit  $\varepsilon \rightarrow 0$  the Dirac  $\delta$  function at the origin which we subtract.

To study the edges of the spectral support we again start from the saddle point equation (20). Multiplying this equation with  $q_0(x)$  and taking the imaginary part for  $x > 0$  we find

$$x \text{Im } q_0(x) = \frac{\gamma^2}{p} \sum_{j=1}^p \frac{\Lambda_j \text{Im } q_0(x)}{(1 + \Lambda_j \text{Re } q_0(x))^2 + \Lambda_j^2 (\text{Im } q_0(x))^2}. \quad (38)$$

A similar equation can be derived for the real part,

$$x \text{Re } q_0(x) = \gamma^2 - 1 - \frac{\gamma^2}{p} \sum_{j=1}^p \frac{1 + \Lambda_j \text{Re } q_0(x)}{(1 + \Lambda_j \text{Re } q_0(x))^2 + \Lambda_j^2 (\text{Im } q_0(x))^2}. \quad (39)$$

The latter equation can be rewritten to

$$\text{Re } q_0(x) = \frac{\gamma^2 - 1 - \gamma^2/p \sum_{j=1}^p 1/[(1 + \Lambda_j \text{Re } q_0(x))^2 + \Lambda_j^2 (\text{Im } q_0(x))^2]}{x + \gamma^2/p \sum_{j=1}^p \Lambda_j/[(1 + \Lambda_j \text{Re } q_0(x))^2 + \Lambda_j^2 (\text{Im } q_0(x))^2]} < 0 \quad (40)$$

which is obviously always negative because  $\gamma^2 = p/n \leq 1$ . Hence the sum  $1 + \Lambda_{j_0} \text{Re } q_0(x)$  might vanish for a particular  $\Lambda_{j_0}$  such that we have to be careful. However this scenario does not happen at an edge where either  $\text{Im } q_0(x) \rightarrow 0$  or  $\text{Im } q_0(x) \rightarrow \infty$  due to the following reason. Suppose  $\text{Re } q_0(x) = -\Lambda_{j_0}^{-1}$  and  $\Lambda_{j_0}$  has the degeneracy  $l_0$ , Eq. (38) then reads

$$x \text{Im } q_0(x) = \frac{\gamma^2}{p} \sum_{\Lambda_j \neq \Lambda_{j_0}} \frac{\Lambda_j \text{Im } q_0(x)}{(1 - \Lambda_j/\Lambda_{j_0})^2 + \Lambda_j^2 (\text{Im } q_0(x))^2} + \frac{\gamma^2 l_0}{p} \frac{1}{\Lambda_{j_0} \text{Im } q_0(x)} \quad (41)$$

which never satisfies one of the two solutions  $\text{Im } q_0(x) = 0, \infty$ . Thus we only have  $1 + \Lambda_j \text{Re } q_0(x) \neq 0$  for all  $j = 1, \dots, p$  at an edge.

For Eq. (38), there are only two types of solutions. Either we are at the origin, then  $\text{Im } q_0(x)$  has to diverge, according to  $\text{Im } q_0(x) = c/\sqrt{x}$  with  $c^{-1} = \gamma^2/p \sum_{j=1}^p 1/\Lambda_j$ , to satisfy Eq. (38), or the edge is not at the origin, then we can expand Eq. (38) for small  $\text{Im } q_0(x)$  which yields the square root behavior

$$\text{Im } q_0(x) \sim \begin{cases} \sqrt{x - x_{\text{edge}}}, & x_{\text{edge}} \text{ is a lower bound of a cut,} \\ \sqrt{x_{\text{edge}} - x}, & x_{\text{edge}} \text{ is an upper bound of a cut.} \end{cases} \quad (42)$$

The largest eigenvalue lies at the edge

$$x_{\text{max}} = g \left( - \int_{-\Lambda_p^{-1}}^0 \Theta(g'(q)) dq \right) \quad (43)$$

with the Heaviside function  $\Theta$ . This result follows from the saddle point equation (20) and from the monotonic behavior of  $g'(x)$ , *cf.* Fig. 1. Accordingly, the smallest eigenvalue lies at the edge

$$x_{\text{min}} = g \left( - \int_{-\infty}^{-\Lambda_1^{-1}} \Theta(-g'(q)) dq - \Lambda_1^{-1} \right). \quad (44)$$

When we have more than only one cut in the spectrum, we find upper bounds at

$$x_{\text{u}}^{(j)} = g \left( \frac{\left( \int_{-\Lambda_{j-1}^{-1}}^{-\Lambda_j^{-1}} \Theta(g'(q)) dq \right)^2 - \int_{-\Lambda_{j-1}^{-1}}^{-\Lambda_j^{-1}} q \Theta(g'(q)) dq}{2 \int_{-\Lambda_{j-1}^{-1}}^{-\Lambda_j^{-1}} \Theta(g'(q)) dq} \right) \quad (45)$$

and lower bounds at

$$x_{\text{l}}^{(j)} = g \left( \frac{\left( \int_{-\Lambda_{j-1}^{-1}}^{-\Lambda_j^{-1}} \Theta(g'(q)) dq \right)^2 + \int_{-\Lambda_{j-1}^{-1}}^{-\Lambda_j^{-1}} q \Theta(g'(q)) dq}{2 \int_{-\Lambda_{j-1}^{-1}}^{-\Lambda_j^{-1}} \Theta(g'(q)) dq} \right) \quad (46)$$

in the interval  $]\Lambda_{j-1}, \Lambda_j[$  with  $j = 2, \dots, p$ . Edges are not found in  $]\Lambda_{j-1}, \Lambda_j[$  when  $x_{\text{u}}^{(j)} = x_{\text{l}}^{(j)}$ , in particular as  $g'(q)$  is strictly negative in  $]-\Lambda_{j-1}^{-1}, -\Lambda_j^{-1}[$ . It might happen that two cuts start merging such that the latter scenario occurs. Then one has to take into account the second derivative  $g''(q)$  and the level density behaves as  $(x_{\text{edge}} - x)^{1/3}$  where we expect Percy kernel [54, 55] behavior on the local scale. We do not show this in the present work.

The situation slightly changes when considering the exact limit  $n, p \rightarrow \infty$  and  $\gamma^2 = p/n$  fixed where we have to assume a limiting density  $\rho(\lambda)$  for the empirical eigenvalues  $\Lambda$ , *cf.* Eq. (16). As long as  $-\text{Re } q_0(x)$  is in the support of the empirical density  $\rho(\lambda)$  where this density is finite we can carry out the same analysis as above because the saddle point solution has to satisfy the counterpart of Eq. (38) which is

$$x \text{Im } q_0(x) = \gamma^2 \int_0^\infty \frac{\lambda \rho(\lambda) d\lambda}{(1 + \lambda \text{Re } q_0(x))^2 + \lambda^2 (\text{Im } q_0(x))^2} \text{Im } q_0(x). \quad (47)$$

As the integrand is non-integrable for  $\text{Im } q_0(x) = 0$  we conclude that  $\text{Im } q_0(x)$  has to be finite. This argument also applies when  $-\text{Re } q_0(x)$  is at an edge of  $\rho(\lambda)$  where the density either diverges (this divergence has to be integrable and to satisfy assumption (14)) or remains finite. Here we exclude the origin where the behavior is different.

When  $-\text{Re } q_0(x)$  is taken at an edge where  $\rho(\lambda)$  vanishes it may happen that  $\text{Im } q_0(x)$  vanishes, too, which is, however, very unlikely. In particular we would expect this scenario only when cuts may start to merge implying that the edge is located in the bulk of the spectrum. The generic case is that  $\text{Im } q_0(x)$  vanishes when  $-\text{Re } q_0(x)$  is outside of the support of the empirical density  $\rho(\lambda)$ . Hence, if this is the case and we are at a soft edge, *i.e.*  $\text{Im } q_0(x) \rightarrow 0$ , we may expand Eq. (47) for small  $\text{Im } q_0(x)$  and find the square root behavior (42).

A hard edge (with  $\text{Im } q_0(x) \rightarrow \infty$ ) of the macroscopic level density (37) only appears at the origin  $x = 0$ . This follows from Eq. (47) when  $\gamma^2 = p/n \rightarrow 1$ . We find the standard  $1/\sqrt{x}$  behavior in the case that  $\rho(\lambda)$  is separated by a finite gap from the origin. The situation drastically changes when the support of  $\rho(\lambda)$  touches the origin. For example for  $\rho(\lambda) = \Theta(1 - \lambda)$  we find a singular behavior with  $\sqrt{\ln x/x}$ . The condition for encountering the standard singularity  $1/\sqrt{x}$  is the existence of the integral  $\int_0^\infty \rho(\lambda) d\lambda/\lambda$ .

We restrict ourselves to a detailed discussion of the soft edges having the form (42) in section IV. On the local scale, we will find the Airy statistics as for the uncorrelated Wishart ensemble.

### C. Correlation Functions

We turn to the  $k$ -point correlations for arbitrary  $k \in \mathbb{N}$ . We may assume that  $x^{(o)} > 0$ ,  $o = 1, \dots, \alpha$  and that these points do not lie at a boundary of the support of the spectral density (37). We thus omit the Dirac  $\delta$  contributions at the origin, in particular the terms  $1/(x_j + iL_j\varepsilon)$  in Eq. (9). We integrate over the non-diagonal supermatrix blocks  $\delta\sigma_{ab}$  ( $a \neq b$ ) which yields a constant equal to  $(2\pi^2)^{2m_a m_b}$  for the block  $\delta\sigma_{ab}$ . We recall that Efetov–Wegner terms do not occur since we only rescale those blocks.

The remaining integrations produce the well-known spectral statistics built upon the sine kernel for real eigenvalues. To show this, we recall — in an appropriate formulation — the integral representation of the  $k$ -point correlation functions on the local scale of a Gaussian Orthogonal Ensemble (GOE) of  $nl \times nl$  real symmetric matrices  $H$ , see [44]

$$\begin{aligned} X_k(\hat{\xi}) &= \lim_{\substack{p \rightarrow \infty \\ \varepsilon \rightarrow 0 \\ j \rightarrow 0}} \sum_{L \in \{\pm 1\}^k} \prod_{i=1}^k \frac{L_i}{4nl} \partial_{j_i} \frac{\int d[H] \exp(-nl \text{tr } H^2) \text{sdet}^{-1/2}(H \otimes \mathbb{1}_{2k|2k} - \mathbb{1}_{nl} \otimes (\pi\hat{\xi}/(nl) + \tilde{j} + i\varepsilon\tilde{L}))}{\int d[H] \exp[-nl \text{tr } H^2]} \\ &= \lim_{\substack{n \rightarrow \infty \\ \varepsilon \rightarrow 0}} K_n \sum_{L \in \{\pm 1\}^k} \int d[\sigma] \exp\left(-\frac{nl}{2} \hat{\mathcal{L}}(\sigma)\right) \prod_{i=1}^k \frac{L_j}{8} \text{str } \sigma \begin{bmatrix} e_{jj}^k & 0 \\ 0 & -e_{jj}^k \end{bmatrix} \otimes \mathbb{1}_2 \end{aligned} \quad (48)$$

where  $\sigma$  is a supermatrix with the same symmetries as in Eq. (5). The Lagrangian is given by

$$\hat{\mathcal{L}}(\sigma) = \frac{1}{2} \text{str } \sigma^2 - i \text{str} \left( i\varepsilon\tilde{L} + \frac{\pi\hat{\xi}}{nl} \right) \sigma - \left( 1 - \frac{1}{nl} \right) \text{str } \ln \sigma. \quad (49)$$

The scaling of the local fluctuations  $\pi\hat{\xi}/(nl)$  is motivated by the local GOE level spacing at the origin. The  $(2k|2k) \times (2k|2k)$  supermatrix  $\sigma$  is integrated over the same domain as in Eq. (5). This  $k$ -point correlation function (48) contains the real sine kernel as can also be derived by other methods such as skew-orthogonal polynomials, *e.g.*, see Refs. [56–58].

The saddle point equation in the limit  $n \rightarrow \infty$  of Eq. (48) is simply  $\sigma = \sigma^{-1}$ . After an analysis similar to the one in subsection III A we find the saddle point manifold  $\sigma = T(\tilde{L} + \delta\sigma/\sqrt{n})T^{-1}$  with  $T \in \text{UOSp}(\tilde{L})/[\text{UOSp}(2k_0|2k_0) \times \text{UOSp}(2k_1|2k_1)]$  where  $\delta\sigma$  is any  $\delta\sigma_{aa}$  in Eq. (33) with  $m^{(a)}$  replaced by  $k$ . The integers  $k_0$  and  $k_1$  are the numbers of +1's and -1's of the  $L_j$ 's, respectively. The Lagrangian (49) becomes

$$\hat{\mathcal{L}}\left(T\tilde{L}T^{-1} + \frac{\delta\sigma}{\sqrt{n}}\right) = \frac{1}{2n} \text{str } \delta\sigma^2 - i \text{str} \left( i\varepsilon\tilde{L} + \frac{\hat{\xi}}{nl} \right) T\tilde{L}T^{-1} + \mathcal{O}\left(\frac{1}{n^{3/2}}\right) \quad (50)$$

which we compare with the approximation (36) of the Lagrangian for the correlated Wishart model. Thus, the identification

$$\hat{\xi}_a^{(o)} = R_1(x^{(o)})\xi_a^{(o)} \quad \Rightarrow \quad d\hat{\xi}_a^{(o)} = R_1(x^{(o)})d\xi_a^{(o)} \quad (51)$$

with  $k \rightarrow m^{(a)}$  must yield the same approximation. Indeed, Eq. (51) is the unfolding prescription to uncover the local spectral fluctuations  $\xi_a^{(o)}$  at the position  $x^{(o)} > 0$ .

To further solidify our line of reasoning, we now show that the remaining parts of the integrand (52) agree with this unfolding. Abbreviating the Efetov–Wegner boundary terms with “b.t.”, we have

$$\begin{aligned}
\lim_{p \rightarrow \infty} R_k(x, \xi) d[\xi] &= \prod_{o=1}^{\alpha} \left[ \frac{K_{\infty, m_o}}{K_{\infty, m_o^{(o)}} K_{\infty, m_1^{(o)}}} d[\xi^{(o)}] \lim_{\varepsilon \rightarrow 0} \sum_{L_1^{(o)}, \dots, L_{m_o}^{(o)} = \pm 1} \int d\mu(T^{(o)}) \right. \\
&\times \prod_{j=1}^{m_o} \frac{L_j^{(o)} \text{Im } q_0(x^{(o)})}{8\pi\gamma^2} \text{str } T^{(o)} \tilde{L}^{(o)} T^{(o)-1} \left[ \begin{array}{cc} e_{jj}^{m_o} & 0 \\ 0 & -e_{jj}^{m_o} \end{array} \right] \otimes \mathbb{1}_2 \\
&\times \exp \left( \frac{i \text{Im } q_0(x^{(o)})}{2\gamma^2} \text{str } \tilde{\xi}^{(o)} T^{(o)} \tilde{L}^{(o)} T^{(o)-1} - \varepsilon \text{str } T^{(o)} \tilde{L}^{(o)} T^{(o)-1} \tilde{L}^{(o)} \right) \Big] + \text{b.t.} \\
&= \prod_{o=1}^{\alpha} X_{m^{(o)}}(\tilde{\xi}_1^{(o)}, \dots, \tilde{\xi}_{m^{(o)}}^{(o)}) d[\tilde{\xi}^{(o)}].
\end{aligned} \tag{52}$$

The ratio of the constants  $K_{\infty, m_o}$ , see Eq. (8), in front of the flat measure  $d[\xi^{(o)}]$  results from the original constant  $K_{nl, k}$  and from the integration over  $\delta\sigma$ . The real parts of  $q_0(x^{(o)})$  drop out because the corresponding integrands are symmetric under the transformation  $T^{(o)} \rightarrow VT^{(o)}$  where  $V$  embeds the supergroup  $\text{UOSp}(2|2)$ . This embedding in the form of a  $(2|2) \times (2|2)$  supermatrix corresponds to the diagonal matrix  $\text{diag}(e_{jj}^{m_o}, e_{jj}^{m_o}; -e_{jj}^{m_o}, -e_{jj}^{m_o})$  which breaks this symmetry for the imaginary parts of  $q_0(x^{(o)})$ . Adjusting Cauchy–like integration theorems *à la* Wegner [34–36, 47–49] to our case of  $\text{UOSp}(2|2)$  we find that the corresponding blocks of  $T^{(o)}$  vanish such that the sign  $L_j$  drops out in the integrand, including the Lagrangian, and the sum over  $L_j$  cancels this contribution. Hence the integral only depends on the imaginary part of the saddle point.

The measure  $d\mu(T^{(o)})$  is the Haar measure on the coset  $\text{UOSp}(\tilde{L}^{(o)})/[\text{UOSp}(2m_o^{(o)}|2m_o^{(o)}) \times \text{UOSp}(2m_1^{(o)}|2m_1^{(o)})]$ . Its normalization is induced by the flat measure  $d[\sigma]$  from which we started. The  $\varepsilon$  term in the exponential function still guarantees absolute convergence of the integral because we may have non–compact group integrals comprised in  $T^{(o)}$ . We absorbed the prefactor in this latter term because we take the limit  $\varepsilon \rightarrow 0$ . The integral over the remaining massive modes  $\delta\sigma$  also yields a constant equal to unity as the numbers of ordinary variables and Grassmann variables are the same.

What is the contribution of the Efetov–Wegner boundary terms in Eq. (52)? — We apply Rothstein’s theory [37] to make changes of variables in superspace. Its main result is that Efetov–Wegner terms can be associated with certain vector fields, here denoted  $\hat{Y}_o$ , see appendix A. For the  $k$ –point correlation function (52), we change the integration variables according to  $\sigma^{(oo)} \rightarrow T^{(o)}(\delta\sigma_{aa}/\sqrt{p} - iq_0(x^{(o)} + i\varepsilon\tilde{L}^{(o)}))T^{(o)-1}$ . Here,  $\sigma^{(oo)}$  is the  $(2m^{(o)}|2m^{(o)}) \times (2m^{(o)}|2m^{(o)})$  supermatrix block of  $\sigma$  which is at the same position in matrix space as  $T^{(o)}(\delta\sigma_{aa}/\sqrt{p} - iq_0(x^{(o)} + i\varepsilon\tilde{L}^{(o)}))T^{(o)-1}$ . Then Eq. (52) becomes

$$\begin{aligned}
\lim_{p \rightarrow \infty} R_k(x; \xi) &= \prod_{o=1}^{\alpha} \left[ K_{\infty, m_o} \lim_{\varepsilon \rightarrow 0} \sum_{L_1^{(o)}, \dots, L_{m_o}^{(o)} = \pm 1} \int \exp[-\hat{Y}_o(T^{(o)}, \delta\sigma_{oo})] d\mu(T^{(o)}) d[\delta\sigma_{oo}] \right. \\
&\times \prod_{j=1}^{m_o} \frac{L_j^{(o)} \text{Im } q_0(x^{(o)})}{8\pi\gamma^2} \text{str } T^{(o)} \tilde{L}^{(o)} T^{(o)-1} \left[ \begin{array}{cc} e_{jj}^{m_o} & 0 \\ 0 & -e_{jj}^{m_o} \end{array} \right] \otimes \mathbb{1}_2 \\
&\times \exp \left( \frac{i \text{Im } q_0(x^{(o)})}{2\gamma^2} \text{str } \tilde{\xi}^{(o)} T^{(o)} \tilde{L}^{(o)} T^{(o)-1} - \varepsilon \text{str } T^{(o)} T^{(o)\dagger} - \frac{l}{4\gamma^2} \text{str } \delta\sigma_{oo}^2 \right) \Big]
\end{aligned} \tag{53}$$

where all Efetov–Wegner boundary terms are taken care of by the vector fields  $\hat{Y}_o(T^{(o)}, \delta\sigma_{oo})$ . Unfortunately, explicit expressions for those vector fields are not available in general. Only for the case of Hermitian supermatrices a successful explicit identification of all Efetov–Wegner boundary terms was achieved in Ref. [41] at small matrix dimension and in Ref. [51] for general supermatrix size. The order of the action of the operators  $\exp[-\hat{Y}_o(T^{(o)}, \delta\sigma_{oo})]$  and the measure  $d\mu(T^{(o)})d[\delta\sigma_{oo}]$  is important since  $d\mu(T^{(o)})$  also incorporates non–trivial ingredients, see appendix A. Hence,  $\hat{Y}_o(T^{(o)}, \delta\sigma_{oo})$  does not only act on the integrand but on this measure, too.

We now can exactly identify the product of integrals (53) with the  $k$ –point correlation function (48). The vector fields  $\hat{Y}_o(T^{(o)}, \delta\sigma_{oo})$  do fully coincide with those for the correlated Wishart ensemble because we perform the same change of integration variables. The integrands are also equal in the large  $p$ –limit, apart from the rescaling of the

spectral fluctuations (unfolding), see Eq. (51). We infer the important result that both correlation functions, including all Efetov-Wegner boundary terms, are exactly the same. The second equality of Eq. (52) reflects the universality of the local spectral fluctuations.

A last remark is in order. The factorization of  $R_k(x)$  into the  $m^{(o)}$ -point correlation functions  $X_{m^{(o)}}(\widehat{\xi}_1^{(o)}, \dots, \widehat{\xi}_{m^{(o)}}^{(o)})$  does not come as a surprise since we zoom into the spectrum at different points  $x^{(1)}, x^{(2)}, x^{(3)}, \dots$ . Those points are macroscopically separated such that eigenvalues around  $x^{(a)}$  should be statistically independent from those around another point  $x^{(b)}$ . This is so because the other infinitely many eigenvalues in between cause a screening. The next to leading order in the  $1/p$  expansion, however, must crucially depend on the random matrix model, especially the confining potential, *e.g.*, see Ref. [59].

#### IV. OUTLIERS AND SOFT EDGES

In subsection IV A we investigate the limiting positions and the fluctuations of possibly existing outliers. In subsection IV B we derive the exact real Airy kernel statistics at any soft edge of the bulk. In subsection IV C we trace back the calculation of the cumulative density function to skew-orthogonal polynomial problem.

##### A. Outliers

An outlier is an eigenvalue that is separated from all other eigenvalues. It thus suffices to investigate the level density (37) because the higher correlations involving outliers are suppressed. We may neglect the outliers in the saddle point equation (20) for the bulk of the eigenvalue density because they are  $1/p$  corrections, but we have to study their average position and the width of their distribution. The peaks in their distribution result from the fact that the saddle point solution  $q_0(x)$  cannot stay on the real line in the vicinity of the poles  $-1/\Lambda_j$ . The solution  $q_0(x)$  has to leave the real line when tuning  $x$ , even though this is only necessary for a very small interval in  $x$ .

We consider the outlier  $\Lambda_o$ , say. To analyze the behavior of the saddle point solution in the presence of  $\Lambda_o$ , we expand the eigenvalue variable  $x = x_0 + \delta x/\sqrt{p}$  and the saddle point  $q_0(x) = -1/\Lambda_o + \delta q_0/\sqrt{p}$  in Eq. (20). The scaling  $1/\sqrt{p}$  for the deviations,  $\delta x$  and  $\delta q_0$ , will turn out to be the correct one later on. The variable  $\delta x$  probes the level density around the point  $x_0$  and, thus, plays the same role as  $\zeta$  in Eq. (3). The point  $x_0$  is the position of the outlier peak for  $p \rightarrow \infty$ , while its corresponding point of the saddle point solution is the pole  $q_0(x_0) = -1/\Lambda_o$ . To express  $x_0$  and  $\delta q_0$  as functions of  $\delta x$ , we expand the saddle point equation (20) up to order  $1/\sqrt{p}$ ,

$$0 \approx \left( -x_0 + \Lambda_o + \frac{\gamma^2}{p} \sum_{j \neq o} \frac{\Lambda_o \Lambda_j}{\Lambda_o - \Lambda_j} \right) + \frac{1}{\sqrt{p}} \left( -\delta x + \Lambda_o^2 \delta q_0 - \frac{\gamma^2}{p} \sum_{j \neq o} \frac{\Lambda_o^2 \Lambda_j^2}{(\Lambda_o - \Lambda_j)^2} \delta q_0 + \frac{\gamma^2}{\delta q_0} \right). \quad (54)$$

This expansion is not valid for the eigenvalues inside a bulk of eigenvalues since then the difference  $\Lambda_o - \Lambda_j$  might be less than order one for some  $j \neq o$ , implying higher order terms in  $p$  in the expansion (54). We now see why the above variations around  $x_0$  and  $q_0 = -1/\Lambda_o$  were chosen of order  $1/\sqrt{p}$  because other dependencies would lead to inconsistent expansions. Identifying the terms of order one and  $1/\sqrt{p}$  yields two results, namely

$$x_0 = \left( 1 + \frac{\gamma^2}{p} \sum_{j \neq o} \frac{\Lambda_j}{\Lambda_o - \Lambda_j} \right) \Lambda_o \quad (55)$$

for the limiting position and

$$\delta q_0(\delta x) = \left( \Lambda_o^2 - \frac{\gamma^2}{p} \sum_{j \neq o} \frac{\Lambda_o^2 \Lambda_j^2}{(\Lambda_o - \Lambda_j)^2} \right)^{-1} \left( \frac{\delta x}{2} \pm \sqrt{\frac{\delta x^2}{4} - \gamma^2 \left( \Lambda_o^2 - \frac{\gamma^2}{p} \sum_{j \neq o} \frac{\Lambda_o^2 \Lambda_j^2}{(\Lambda_o - \Lambda_j)^2} \right)} \right) \quad (56)$$

for the deviation of the saddle point solution from the pole  $q_0 = -1/\Lambda_o$ . Interestingly, the position of the outlier is not directly at  $\Lambda_o$  but slightly shifted, *cf.*, Eq. (55). Only in the limit  $p \gg 1$  and  $\Lambda_o \gg \Lambda_j$  for all  $\Lambda_j$  in the bulk of the eigenvalues, we have  $x_0 = \Lambda_o$ .

The fluctuations of the outlier around the position  $x_0$  are of the order

$$\Delta x_0 \approx 2\gamma \sqrt{1 - \frac{\gamma^2}{p} \sum_{j \neq o} \frac{\Lambda_j^2}{(\Lambda_o - \Lambda_j)^2} \frac{\Lambda_o}{\sqrt{p}}} \quad (57)$$

as can be read off from the relation between the level density (37) and the saddle point  $q_0$ . The saddle point only yields a contribution to the spectral density if it has a non-vanishing imaginary part which, in turn, can only result from the square root in Eq. (56). This implies a condition on the empirical eigenvalues for the expansion (54) to hold,

$$\frac{\gamma^2}{p} \sum_{j \neq o} \frac{\Lambda_j^2}{(\Lambda_o - \Lambda_j)^2} < 1. \quad (58)$$

This condition can occasionally be violated for some time series as we show in our numerical simulations in section V. In such cases the expansion (54) fails because the matrix dimensions are too small. We expect that the condition (58) is always true for sufficiently large  $p$  and  $n$  and for an outlier  $\Lambda_o$  that is larger than the soft edge of the bulk. This is consistent with the  $1/p$  suppression of the contribution due to other outliers in the sum (58). If  $p, n$  are too small, the condition (58) fails whenever  $(\Lambda_o - \Lambda_a)^2 \leq \Lambda_a^2/n$  with  $\Lambda_a$  being another outlier. The difference  $(\Lambda_o - \Lambda_a)$  then has an order  $\sqrt{p}$  behavior, resulting in a higher order polynomial equation for the saddle points. Another problem arises when the outlier is too close to a soft edge of a bulk of eigenvalues. Such a situation can emerge when the noise in the data becomes too strong and the outliers start to merge with the bulk. Again, the saddle point equation has to be modified. The worst scenario is when both situations occur simultaneously.

Another point deserves further discussion. The square root behavior of the level density, also known from Wigner's semi-circle law, cannot be interpreted as the limiting distribution of the outlier. A simple argument from the full random matrix model (1) shows that, for large  $p$  and fixed degeneracy  $l$ , the distribution for the outlier around  $\Lambda_o$  coincides with the level density of the  $l \times l$  Gaussian Orthogonal Ensemble (GOE) centered at  $x_0$  and with fluctuations proportional to  $\Delta x_0$ . The shape of the outlier level density encodes the number of eigenvalues, *i.e.*, the degeneracy  $l$ , Fig. 3. Nonetheless the position and the widths of the distributions of the outliers are still the same. Only in the limit  $l \rightarrow \infty$  of infinite degeneracy we find Wigner's semi-circle law again. The reason for this behavior is the macroscopic distance of the bulk and the outlier. The distributions of the individual eigenvalues of the outlier (indeed we have more than one because of the degeneracy  $l$ ) with those in the bulk will only have an exponentially small overlap such that one can consider the eigenvalues in the outlier separately.

Interestingly, the results (55) and (57) seem also applicable to outliers which lie on a scale different from that of the bulk. The limiting position  $x_0$  as well as the order  $\Delta x_0$  of fluctuations scale with  $\Lambda_o$ . They are thus likely to become  $x_0 = \Lambda_o$  and  $\Delta x_0 \approx 2\gamma\Lambda_o/\sqrt{p}$  for large  $p$ .

## B. Airy Statistics at the Soft Edges

We restrict ourselves to the soft edges where the asymptotic level density (37) vanishes as a square root and derive the Airy kernel. We do not consider higher order multi-critical points which cannot be excluded *a priori*. For the sake of simplicity we assume that  $x_j = x_0$  for all  $j = 1, \dots, k$  coincides with the position where the level density (37) vanishes. Then we have only one saddle point  $Q_0 = q_0(x_0)\mathbb{1}_{2k|2k}$ . We recall that  $q_0(x_0)$  starts to become real at the edge  $x_0$  such that it does not have an imaginary part that is related to the metric  $\tilde{L}$ . The scale of the local fluctuations  $\xi$  changes to  $\tilde{\kappa} = x_0\mathbb{1}_{2k|2k} + \tilde{j} + \xi/(lp)^{2/3} + \imath\tilde{L}\varepsilon$ , employing the notation of Eq. (5). This scale reflects the fact that the level density vanishes like a square root and that one has to expand around the saddle point up to third order. The massive modes  $\delta\sigma$  around the saddle point solution scales differently, too, in particular we have the expansion  $\sigma = -\imath q_0(x_0)\mathbb{1}_{2k|2k} + \delta\sigma/(lp)^{1/3}$ . On the scale of the local fluctuations, we take into account the position of the outlier and expand the Lagrangian (10) up to order  $1/p$ ,

$$\begin{aligned} & \mathcal{L} \left( x_0\mathbb{1}_k + \frac{\xi}{(lp)^{2/3}}, -\imath q_0\mathbb{1}_{2k|2k} + \frac{\delta\sigma}{(lp)^{1/3}} \right) \\ &= \frac{\imath}{(lp)^{1/3}} \left[ \frac{\gamma^2}{p} \sum_{i=1}^p \frac{\Lambda_i}{1 + \Lambda_i q_0} - x_0 - \frac{1}{q_0} \right] \text{str} \delta\sigma + \frac{1}{2(lp)^{2/3}} \left[ \frac{\gamma^2}{p} \sum_{i=1}^p \frac{\Lambda_i^2}{(1 + \Lambda_i q_0)^2} - \frac{1}{q_0^2} \right] \text{str} \delta\sigma^2 \\ & \quad - \frac{\imath}{3lp} \text{str} \left[ \left( \frac{\gamma^2}{p} \sum_{i=1}^p \frac{\Lambda_i^3}{(1 + \Lambda_i q_0)^3} - \frac{1}{q_0^3} \right) \delta\sigma^3 + 3(\tilde{\xi} + \imath(lp)^{2/3}\varepsilon\tilde{L})\delta\sigma \right] + \mathcal{O} \left( \frac{1}{(lp)^{4/3}} \right). \end{aligned} \quad (59)$$

The term of order  $\mathcal{O}(p^0) = \mathcal{O}(1)$  drops out because the saddle point is proportional to the identity matrix such that the corresponding supertraces vanish. Moreover the terms of order  $1/(lp)^{1/3}$  and  $1/(lp)^{2/3}$  vanish because  $q_0(x_0)$  is the contributing saddle point at the position  $x_0$  where the level density vanishes in a square-root fashion. The first term of Eq. (59) is the function  $\hat{g}(q(x), x)$  appearing in the scalar saddle point equation (20), while the second term is its derivative  $g'(q)$  with respect to the variable  $q$ . We underline that the derivative  $\partial_q \hat{g}(q, x) = g'(q)$  vanishes at  $q_0$ ,

too, which can be seen as follows. On the one hand,  $R_1(x)$  vanishes as  $\sqrt{|x-x_0|}$  such that the Cauchy transform of  $R_1(x)$ , which is up to normalization the saddle point solution  $q_0$ , has a divergent first derivative at  $x = x_0$ , i.e.,  $q'(x) \rightarrow 1/\sqrt{|x-x_0|} \rightarrow \infty$  for  $x \rightarrow x_0$ . On the other hand the total derivative of the function  $\hat{g}(q_0(x), x)$  in the variable  $x$  yields  $0 = d\hat{g}/dx(q_0(x), x) = -1 + g'(q_0(x))q'_0(x)$  which indeed has to vanish because  $q_0$  is the saddle point solution. Thus we have  $g'(q_0(x)) = 1/q'_0(x)$  implying that  $g'$  vanishes at  $q_0(x_0)$ .

The  $1/p$  term in Eq. (59) is the leading term of the Lagrangian. Thus the  $k$ -point correlation function at the edge  $x_0$  takes the form

$$R_k(x_0, (lp)^{1/3}\xi)d[(lp)^{1/3}\xi] \stackrel{p \gg 1}{\approx} K_n \lim_{\varepsilon \rightarrow 0} \sum_{L_1, \dots, L_k = \pm 1} \int d[\delta\sigma] \prod_{j=1}^k \frac{L_j}{8\pi i \gamma^2} \text{str} \delta\sigma \begin{bmatrix} e_{jj}^k & 0 \\ 0 & -e_{jj}^{m_o} \end{bmatrix} \otimes \mathbb{1}_2 \\ \times \exp \left( \frac{i}{6\gamma^2} \text{str} \left[ \left( \frac{\gamma^2}{p} \sum_{i=1}^p \frac{\Lambda_i^3}{(1 + \Lambda_i q_0(x_0))^3} - \frac{1}{q_0^3(x_0)} \right) \delta\sigma^3 + 3(\tilde{\xi} + i(lp)^{2/3}\varepsilon\tilde{L})\delta\sigma \right] \right). \quad (60)$$

We reiterate that Efetov–Wegner boundary terms and, hence, non-vanishing vector fields à la Rothstein [37] do not appear. The coordinate transformation is only a constant shift that cannot cause such contributions. The terms where we replace  $\delta\sigma$  or its higher powers by the leading order saddle point solution  $i q_0(x_0) \mathbb{1}_{2k|2k}$  inside the product of the integrand in Eq. (60) vanish for the same reason as in the bulk, see the discussion below Eq. (52). The integral turns out invariant under the sub-supergroup  $\text{UOSp}(2|2)$  such that Cauchy-like Wegner integration theorems [35, 47–49] apply which reduce the integral over the supermatrix  $\delta\sigma$  to an integral over a supermatrix of a smaller dimension. Then one of the signs  $L_j$  drop out and, thus, the remaining integrand is independent of the sign of the imaginary increment over which the sum runs. Precisely this sum yields zero due to the additional alternating signs  $L_j$  in the product.

The limit  $\varepsilon \rightarrow 0$  together with the sign matrix  $\tilde{L}$  and, thus, the original domain of integration of  $\sigma$  fixes the integration contour for the eigenvalues of the boson–boson and fermion–fermion blocks of  $\delta\sigma$ . The contour for an eigenvalue  $s_{B,j}$  in the boson–boson block consists of two disjoint half-lines and is equal to the union  $-i\mathbb{R}_+ \cup L_j\mathbb{R}_+$ . We emphasize that the integration over  $-i\mathbb{R}_+$  results from the negative sign of  $q_0(x_0)$  implying that the saddle point  $-i q_0(x_0)$  lies on the positive half-axis. The integrability of  $-i\mathbb{R}_+$  is ensured by the cubic term, and the integration over  $L_j\mathbb{R}_+$  is absolutely convergent due to the  $\varepsilon$  term. When tilting the second half-line to  $L_j\mathbb{R}_+ \rightarrow (L_j/2 + \sqrt{3}i/2)\mathbb{R}_+$  we can perform the  $\varepsilon \rightarrow 0$  limit exactly, because in this more appropriate integration domain the cubic term dominates on both half-lines. The integration over an eigenvalue  $s_{F,j}$  in the fermion-fermion block consists of the two half-lines  $e^{i7\pi/6}\mathbb{R}_+ \cup e^{i11\pi/6}\mathbb{R}_+$  independent of  $\tilde{L}$ .

Again we have to unfold the local fluctuations which leads to

$$\widehat{\xi}_a^{(o)} = \left( \frac{\gamma^2}{p} \sum_{i=1}^p \frac{\Lambda_i^3}{(1 + \Lambda_i q_0(x_0))^3} - \frac{1}{q_0^3(x_0)} \right)^{-1/3} \frac{\xi_a}{\gamma^{4/3}}. \quad (61)$$

To obtain  $k$ -point correlations, we also have to rescaled the supermatrix  $\delta\sigma$  and arrive at

$$\lim_{p \rightarrow \infty} R_k(x_0, (lp)^{1/3}\xi)d[\xi] = K_{\infty,k} d[\widehat{\xi}] \sum_{L_1, \dots, L_k = \pm 1} \int d[\delta\sigma] \exp \left( \frac{i}{6} \text{str} \left[ \delta\sigma^3 + 3\widehat{\xi}\delta\sigma \right] \right) \prod_{j=1}^k \frac{L_j}{8\pi i} \text{str} \delta\sigma \begin{bmatrix} e_{jj}^k & 0 \\ 0 & -e_{jj}^{m_o} \end{bmatrix} \otimes \mathbb{1}_2. \quad (62)$$

The asymptotic result (62) can be written in terms of the Airy kernel and is thus equivalent to the result for the GOE [60]. We recall that the GOE is well-known to exhibit Airy statistics at the soft edges. We choose the local

scaling limit of the corresponding  $k$ -point correlation functions at the edge  $x_0 = 2$  and find

$$\begin{aligned}
\widehat{X}_k(\widehat{\xi})d[\widehat{\xi}] &= d[\widehat{\xi}] \lim_{\substack{p \rightarrow \infty \\ \varepsilon \rightarrow 0 \\ j \rightarrow 0}} \sum_{L \in \{\pm 1\}^k} \prod_{i=1}^k \frac{L_i}{4i\pi nl} \partial_{j_i} \\
&\times \frac{\int d[H] \exp(-nl \operatorname{tr} H^2) \operatorname{sdet}^{-1/2}(H \otimes \mathbb{1}_{2k|2k} - \mathbb{1}_{nl} \otimes (2\mathbb{1}_{2k|2k} + \widehat{\xi}/(nl)^{2/3} + \tilde{j} + i\varepsilon\tilde{L}))}{\int d[H] \exp[-nl \operatorname{tr} H^2]} \\
&= d[\widehat{\xi}] \lim_{\substack{n \rightarrow \infty \\ \varepsilon \rightarrow 0}} K_n \sum_{L \in \{\pm 1\}^k} \int d[\sigma] \exp\left(-\frac{nl}{2} \widehat{\mathcal{L}}(\sigma)\right) \prod_{i=1}^k \frac{L_j}{8} \operatorname{str} \sigma \begin{bmatrix} e_{jj}^k & 0 \\ 0 & -e_{jj}^k \end{bmatrix} \otimes \mathbb{1}_2 \\
&= \lim_{p \rightarrow \infty} R_k(x_0, (lp)^{1/3} \xi) d\left[(lp)^{1/3} \xi\right]
\end{aligned} \tag{63}$$

with

$$\widehat{\mathcal{L}}(\sigma) = \frac{1}{2} \operatorname{str} \sigma^2 - i \operatorname{str} \left( i\varepsilon\tilde{L} + \frac{\widehat{\xi}}{(nl)^{2/3}} \right) \sigma - \left( 1 - \frac{1}{nl} \right) \operatorname{str} \ln \sigma. \tag{64}$$

To arrive at the last equality of Eq. (63) we expanded the supermatrix according to  $\sigma = i\mathbb{1}_{2k|2k} + \delta\sigma/(nl)^{2/3}$  and identified the result with the right hand side of Eq. (62). Of course, the edge correlations of the GOE can be also derived by other methods, *e.g.* orthogonal polynomials. We conclude that the correlated real Wishart ensemble (1) shows, at any soft edge that behave in a square-root fashion, spectral correlations of the Airy type known from the GOE.

### C. Distribution of the Largest Eigenvalue

We consider a particular example to illustrate how useful the independence of the correlations and densities in the limit of large matrix dimensions is. In particular, it leads to simpler analytical results. We study the cumulative density function for the largest eigenvalue of the correlated Wishart matrix  $WW^T$ . As we have shown that the soft edges as well as the outliers are independent of the generic degeneracy of the empirical correlation matrix  $C$  in the limit of large matrix dimension, we expect that this also hold approximately for the position and the width of the largest-eigenvalue distribution. If outliers are not present and the largest eigenvalue lies at the upper soft edge we find the Tracy–Widom distribution [60]. Later on, we will present numerical simulations which confirm that, in first approximation, the distribution for the largest eigenvalue of the bulk of the eigenvalues indeed shows the expected behavior, see Fig. 4.

The cumulative density function for the largest eigenvalue of the correlated real Wishart ensemble with a generic degeneracy  $l = 2$  in the empirical correlation matrix  $C \otimes \mathbb{1}_2$  is given by

$$E_{2p,n}(t) = \int d[W] P(W|C \otimes \mathbb{1}_2) \Theta(t\mathbb{1}_{2p} - WW^T), \tag{65}$$

where  $\Theta$  is the Heaviside function on the symmetric matrices, *i.e.*, it is unity if the matrix is positive definite and zero otherwise. The function  $E_{2p,n}(t)$  may also be viewed as the gap probability that none of the eigenvalue is larger than  $t \in \mathbb{R}_+$ . Its derivative with respect to  $t$  yields the distribution of the largest eigenvalue. In Ref. [17] we have shown that such integrals can be mapped to invariant symmetric matrix ensembles. Then the cumulative density function (65) can be rewritten as an integral over a  $2n \times 2n$  real symmetric matrix  $H$ , namely

$$E_{2p,n}(t) = \left(\frac{nt}{2}\right)^{2np} \frac{K'_{n,n}}{\det^{2n} \Lambda} \int \frac{\exp[\operatorname{tr}(iH + \mathbb{1}_{2n})] d[H]}{\det^{(2n+1)/2}(iH + \mathbb{1}_{2n}) \prod_{j=1}^p \det(iH + (nt\Lambda_j^{-1}/2 + 1)\mathbb{1}_{2n})}. \tag{66}$$

The limit  $E_{2p,n}(t \rightarrow \infty) = 1$  yields the normalization constant

$$\frac{1}{K'_{j,n}} = \int \frac{\exp[\operatorname{tr}(iH + \mathbb{1}_{2j})] d[H]}{\det^{(2n+1)/2}(iH + \mathbb{1}_{2j})} = \prod_{a=0}^{2j-1} \frac{2\pi^{(a+2)/2}}{\Gamma[(2n-a+1)/2]} \tag{67}$$

which is a special form of the Ingham-Siegel integral [62, 63].

Without the degeneracies, the square roots of the determinants  $\det(\imath H + (nt\Lambda_j^{-1}/2 + 1)\mathbb{1}_{2n})$  in the integrand (66), *cf.* Ref. [17], would be most cumbersome. Luckily, the double degeneracy of each empirical eigenvalues combines two square roots and yields a determinant to power one. This is a considerable advantage as compared to the non-degenerated case. Hence, we can algebraically reformulate the integrand such that the integral drastically simplifies. To this end, we diagonalize the matrix  $H = OEO^T$  with  $O \in \text{SO}(2n)$  and  $E = \text{diag}(E_1, \dots, E_{2n}) \in \mathbb{R}^{2n}$ ,

$$E_{2p,n}(t) = \left(\frac{nt}{2}\right)^{2np} \frac{\tilde{K}_{n,n}}{(2n)! \det^{2n} \Lambda} \int \frac{\exp[\text{tr}(\imath E + \mathbb{1}_{2n})] |\Delta_{2n}(E)| d[E]}{\det^{(2n+1)/2}(\imath E + \mathbb{1}_{2n}) \prod_{j=1}^p \det(\imath E + (nt\Lambda_j^{-1}/2 + 1)\mathbb{1}_{2n})} \quad (68)$$

where the intergration over the orthogonal group [56] leads to the new normalization constant

$$\frac{1}{\tilde{K}_{j,n}} = \frac{1}{K'_{j,n}} \prod_{a=0}^{2j-1} \frac{2\Gamma[(a+3)/2]}{\pi^{(a+1)/2}} = \prod_{a=1}^{2j} \frac{4\sqrt{\pi}\Gamma[(a+2)/2]}{\Gamma[(2n-a+2)/2]} = \prod_{a=1}^j \frac{2^{2n-4a+5}\pi(2a)!}{(2n-2a+1)!} \quad (69)$$

Algebraic rearrangement [64] and the usage of skew-orthogonal polynomials [57, 58] uncovers the Pfaffian structure of the integral (68),

$$E_{2p,n}(t) = \frac{\tilde{K}_{n,n}}{\tilde{K}_{n-p/2,n}} \frac{\text{Pf}[\mathcal{K}_n(nt\Lambda_a^{-1}/2, nt\Lambda_b^{-1}/2)]_{a,b=1,\dots,p}}{\det(2\Lambda/(nt))^{2n} \Delta_p(nt\Lambda^{-1}/2)} \quad (70)$$

with the kernel

$$\mathcal{K}_n(x_1, x_2) = \frac{1}{i} \left( \int \frac{dE_1 dE_2 \text{sign}(E_1 - E_2)}{(\imath E_1 + x_1 + 1)(\imath E_2 + x_2 + 1)} \frac{\exp(\imath E_1 + \imath E_2 + 2)}{(\imath E_1 + 1)^{(2n+1)/2} (\imath E_2 + 1)^{(2n+1)/2}} \right. \\ \left. - \sum_{l=0}^{p/2-1} \frac{\hat{q}_{2l}(x_1)\hat{q}_{2l+1}(x_2) - \hat{q}_{2l}(x_2)\hat{q}_{2l+1}(x_1)}{h_l} \right). \quad (71)$$

This result is only true for  $p$  even. For  $p$  odd we may augment the empirical eigenvalues  $\Lambda$  with a dummy eigenvalue  $\Lambda_{p+1}$  such that we effectively extend  $p \rightarrow p+1$  and eventually take the limit  $\Lambda_{p+1} \rightarrow \infty$ . We refrain from showing the details and stick to the case of  $p$  even in the sequel. The functions  $\hat{q}_l(x)$  in Eq. (71) are the Cauchy transforms

$$\hat{q}_l(x) = \int \frac{dE_1 dE_2 \text{sign}(E_1 - E_2) q_l(E_1)}{\imath E_2 + x + 1} \frac{\exp(\imath E_1 + \imath E_2 + 2)}{(\imath E_1 + 1)^{(2n+1)/2} (\imath E_2 + 1)^{(2n+1)/2}}, \quad (72)$$

of the skew-orthogonal polynomials  $q_l(E)$  (in monic normalization) according to

$$\int dE_1 dE_2 \text{sign}(E_1 - E_2) q_{2a}(E_1) q_{2b+1}(E_2) \frac{\exp(\imath E_1 + \imath E_2 + 2)}{(\imath E_1 + 1)^{(2n+1)/2} (\imath E_2 + 1)^{(2n+1)/2}} = h_a \delta_{ab}, \quad (73)$$

with  $a, b \in \mathbb{N}_0$ . All other bilinear relations between the polynomials vanish. The constants  $h_a$  follow from the normalization constant (69),

$$\frac{1}{\tilde{K}_{j,n}} = \prod_{l=0}^{j-1} h_l \quad \longleftrightarrow \quad h_j = \frac{\tilde{K}_{j,n}}{\tilde{K}_{j+1,n}} = \frac{2^{2n-4j+1}\pi(2j-2)!}{(2n-2j-1)!}. \quad (74)$$

The Cauchy transform  $\hat{q}_l(x)$  is readily derived as a Heine-type-of formula [38]

$$\hat{q}_{2l}(x) = \frac{h_l K'_{l+1,n}}{i^{2l+1} (2l+2)!} \int \frac{\exp[\text{tr}(\imath H + \mathbb{1}_{2l+2})] d[H]}{\det^{(2n+1)/2}(\imath H + \mathbb{1}_{2l+2}) \det(\imath H + (x+1)\mathbb{1}_{2l+2})} \quad (75)$$

and

$$\hat{q}_{2l+1}(x) = -\frac{h_l K'_{l+1,n}}{i^{2l} (2l+2)!} \int \frac{(x + i \text{tr} H + c_l) \exp[\text{tr}(\imath H + \mathbb{1}_{2l+2})] d[H]}{\det^{(2n+1)/2}(\imath H + \mathbb{1}_{2l+2}) \det(\imath H + (x+1)\mathbb{1}_{2l+2})} \quad (76)$$

with an arbitrary constant  $c_l$  which cannot be fixed with the skew-orthogonality relation but can be used as a gauge parameter. The matrix  $H$  is a  $(2l+2) \times (2l+2)$  real symmetric matrix.

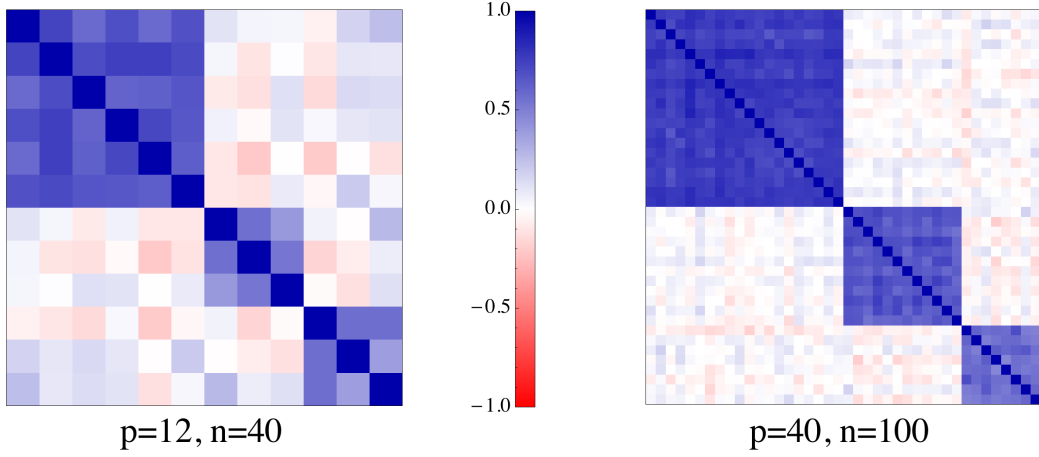


FIG. 2: The two empirical correlation matrices of a  $12 \times 40$  time series (left plot) and a  $40 \times 100$  time series (right plot) which were employed for the Monte Carlo simulations. The strength of the correlation is color coded as shown in the legend.

The integral (75) is very similar to the gap probability  $E_{p=1,n}(t=1)$  at  $t=1$ , *cf.*, Eq. (66), with the empirical correlation matrix  $C^{-1} \rightarrow 2x/n$ , in particular we have

$$\widehat{q}_{2l}(x) = \frac{(-1)^l h_l}{i\pi^{2n}} x^{2(n-l)-2} \int d[W] \exp[-x \text{tr} WW^T] \det^{2n-2l-2}(\mathbb{1}_2 - WW^T) \Theta(\mathbb{1}_2 - WW^T) \quad (77)$$

with  $W$  a  $2 \times 2n$  real matrix. The Cauchy transform  $\widehat{q}_{2l+1}(x)$  of the odd polynomials can also be expressed in terms of such an integral, as it can be traced back to a derivative of  $\widehat{q}_{2l}(x)$ ,

$$\widehat{q}_{2l+1}(x) = -i \left( x + c_l - 2i(l+1) + 2(l+1)(n-l) + x \frac{\partial}{\partial x} \right) \widehat{q}_{2l}(x). \quad (78)$$

Setting  $c_l = 2i(l+1) - 2(l+1)(n-l)$  we have

$$\begin{aligned} \widehat{q}_{2l+1}(x) &= -ix \left( 1 + \frac{\partial}{\partial x} \right) \widehat{q}_{2l}(x) \\ &= \frac{(-1)^{l+1} h_l}{\pi^{2n}} x^{2(n-l)-1} \int d[W] (1 - \text{tr} WW^T) \exp[-x \text{tr} WW^T] \det^{2n-2l-2}(\mathbb{1}_2 - WW^T) \Theta(\mathbb{1}_2 - WW^T), \end{aligned} \quad (79)$$

where  $W$  is a real  $2 \times 2n$  matrix. We point out that the imaginary unit in Eq. (77) cancels with the one in the kernel (71) such that the result is indeed as required. The integral (77) can be evaluated in closed form by diagonalizing the  $2 \times 2$  Wishart correlation matrix  $WW^T$  and integrating over the corresponding two eigenvalues. This yields the finite sum

$$\begin{aligned} \widehat{q}_{2l}(x) &= \frac{(-1)^l h_l (6n-4l-5)!}{i 2^{4(n-l-1)} (2n-2)!} \frac{1}{x^{4n-2l-2}} \sum_{b=0}^{2(n-l-1)} \binom{2(n-l-1)}{b} \\ &\quad \times \frac{{}_2F_1(3/2-n, 1+b; 2+b; -1)}{(2^{n+1/2}-2)(1+b)} {}_1F_1(2(b-2n+2l+2); 4l-6n+4; 2x). \end{aligned} \quad (80)$$

The functions  ${}_1F_1$  and  ${}_2F_1$  are the confluent and Gauss' hypergeometric functions, respectively. The functions  $\widehat{q}_{2l+1}(x)$  can be evaluated via relation (79), we omit the details.

Altogether, we derived the rather simple and fairly explicit results (70), (71), (74), (79) and (80) for the cumulative distribution of the largest eigenvalue of  $WW^T$  in the presence of degeneracies in  $C$  ( $l=1$ ), *cf.* Ref. [17]. Without degeneracies, non-trivial analytical problems arise due to the square roots of determinants. Applying now our observation that the spectral statistics become the same for large time series, our above results asymptotically solve the corresponding problem without degeneracies. Hence, we developed a general method to obtain asymptotic results for other quantities of the correlated real Wishart ensemble by artificially introducing double degeneracies in the empirical correlation matrix  $C$ .

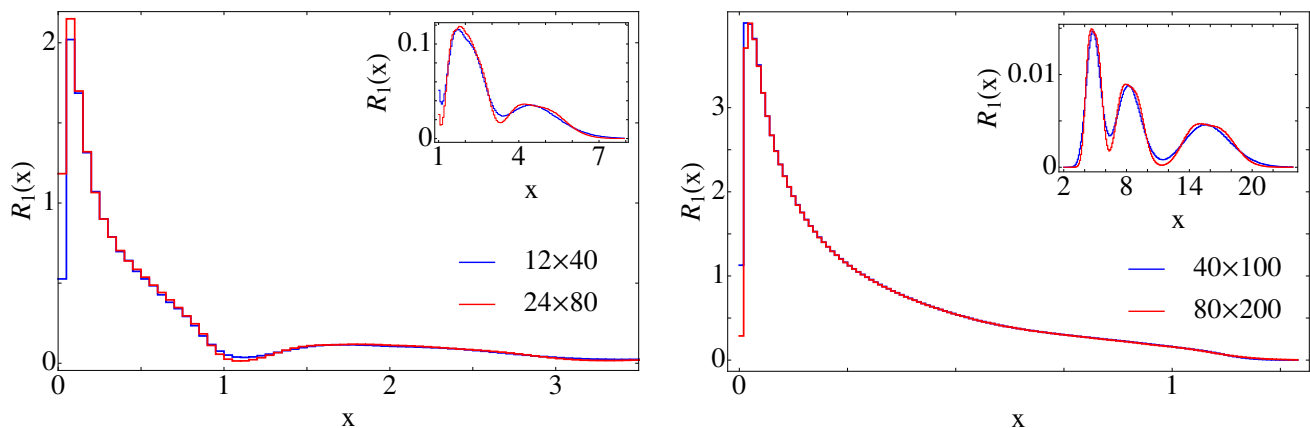


FIG. 3: Level densities as histograms for the real Wishart ensembles with the two empirical correlation matrices shown in Fig. 2. Blue lines correspond to the non-degenerated and red lines to the doubly degenerate empirical correlation matrices. The level densities around the outliers are shown on a magnified scale in the insets.

## V. NUMERICAL SIMULATIONS

For illustrating purpose and to show the robustness of our approximations and predictions, we carry out two Monte Carlo simulations of the correlated real Wishart ensemble (1). We use a one-factor model, see *e.g.* Ref. [?], to construct two sets of time series  $T_{12 \times 40}$  ( $p = 12$  and  $n = 40$ ) and  $T_{40 \times 100}$  ( $p = 40$  and  $n = 100$ ). Each set  $T = T_0 + s_{\text{noise}} T_1$  consist of a signal  $T_0$  featuring three perfectly correlated sectors and a fully uncorrelated white-noise offset  $T_1$  such that  $\langle \{T_1\}_{ab} \rangle = 0$  and  $\langle \{T_1\}_{ab} \{T_1\}_{a'b'} \rangle = \delta_{aa'} \delta_{bb'}$ . The strength of the noise is tuned by the parameter  $s_{\text{noise}}$ . In the simulations we choose  $s_{\text{noise}} = 3$  for  $T_{12 \times 40}$  and as  $s_{\text{noise}} = 4$  for  $T_{40 \times 100}$ . From these sets of times series we derive the corresponding empirical correlation matrices  $C_{12 \times 40}$  and  $C_{40 \times 100}$ . They are shown in Fig. 2. The three strongly correlated sectors show up as deep blue blocks on the diagonal although the white noise is of the same order as the signal. The sizes of these blocks,  $(6, 3, 3)$  for  $T_{12 \times 40}$  and  $(20, 12, 8)$  for  $T_{40 \times 100}$ , mainly determine the positions of three largest eigenvalues (outliers) of the corresponding empirical correlation matrices,  $\Lambda_{12 \times 40}^{(\text{out})} \approx \text{diag}(4.44, 2.17, 2.03)$  for  $T_{12 \times 40}$  and  $\Lambda_{40 \times 100}^{(\text{out})} \approx \text{diag}(15.61, 8.39, 5.08)$  for  $T_{40 \times 100}$ . However, we see strong shifts in Fig. 3 (left) for the smaller time series  $T_{12 \times 40}$  because of the relatively strong noise and the relatively small matrix dimensions.

We numerically simulate the real Wishart ensemble for each of these two so constructed empirical correlation matrices  $C_{12 \times 40}$  and  $C_{40 \times 100}$  and their doubly degenerate counter parts  $C_{12 \times 40} \otimes \mathbb{1}_2$  and  $C_{40 \times 100} \otimes \mathbb{1}_2$ . Altogether we simulate four ensembles. The ensembles consist of  $10^6$  matrices for each empirical correlation matrix. These large ensemble sizes lead to high statistical significance. In Fig. 3, we present the macroscopic level densities including outliers, the statistical errors amount to a few percents at most. The level densities employing the degenerate and non-degenerate empirical correlation matrices show perfect agreement in the bulk of the empirical eigenvalues. Not surprisingly, the agreement is better for larger dimension  $p$ . Nevertheless, even for low matrix dimensions  $p$  and  $n$ , the deviations in the bulk are small. At the edges and for the outliers the deviations become visible beyond the statistical error. They result from the statistical fluctuations of the individual eigenvalues around their average positions due to the level repulsion caused by the overlapping tails of the individual eigenvalue distributions which are still present at finite matrix dimension. In the bulk the eigenvalues are more abundant, implying that their respective positions are sharper. In contrast, the eigenvalues near the soft edges explore the region outside the limiting support, while they strongly accumulate at the hard edge as the cross-over to the negative real line is forbidden. This behavior is suppressed by a generic degeneracy in the empirical correlation matrix. Although the empirical correlation matrix might be degenerate, the corresponding Wishart correlation matrix  $WW^T$  is not. Hence there are for the doubly degenerate matrix twice as many eigenvalues in  $WW^T$  as in the non-degenerate case. This implies that the degenerate case is closer to the asymptotic result (37) derived by the saddle point solution. In particular, the support becomes more restrictive. The same discussion also applies to the outliers whose overlaps with the other eigenvalues are more suppressed when the empirical correlation matrix is doubly degenerate. We notice that the level densities around the outliers only reaches values of up to two orders smaller than in the bulk.

Although the level density of the bulk exhibits the strongest differences at its edges, the spectral statistics on the local scale converges surprisingly well for the Wishart ensembles with and without the degeneracies in the empirical

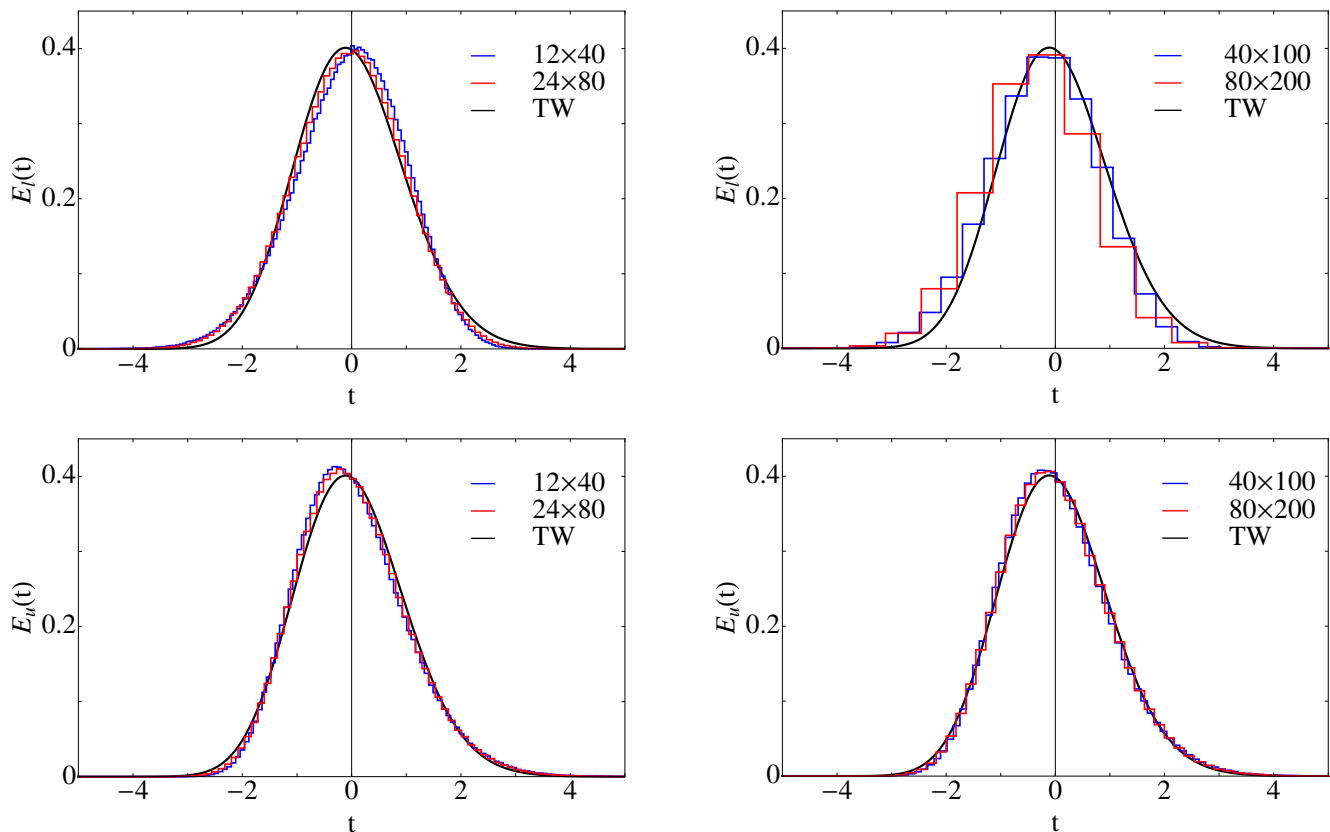


FIG. 4: The distributions of the smallest ( $E_l(t)$ , top row) and of the largest ( $E_u(t)$ , bottom row) eigenvalues of the bulk normalized to zero mean and variance one. We consider again the same ensemble of Fig. 3 with the  $12 \times 40$  correlation matrix (left column) and the  $40 \times 100$  correlation matrix (right column) of Fig. 2. The histograms for the non-degenerate (blue) and the doubly degenerate (red) empirical correlation matrix are also compared to approximations (81) for the Tracy-Widom distribution (black smooth curve, TW) for real matrices. The agreement with the limiting Tracy-Widom distribution is astoundingly good and even the leading order in the deviations from this distribution seem to be independent of the degeneracy.

correlation matrices. This is seen in Fig. 4 which displays the distribution of the largest and smallest eigenvalue at the edges of the bulk. For the comparison, the numerical results are unfolded such that the distributions have zero mean and unit variance. Moreover, the distributions of the smallest eigenvalue are mirrored at the origin to compare the numerical results with the Tracy–Widom distribution [60] for real matrices which should be the limiting distribution for large matrix dimensions  $p$  and  $n$ . The Tracy–Widom distribution indicates that the Airy statistics holds in this regime. We employed the approximation

$$E_{\text{TW}}(t) \approx 6.68 \times 10^{-76} (t + 8.93)^{78.66} \exp(-8.93t), \quad t > -8.93, \quad (81)$$

of the Tracy–Widom distribution [61]. Again, this distribution was normalized to zero mean and unit variance. The agreement with the Tracy–Widom distribution is quite good despite the small matrix dimensions  $p = 12, 40$  in our numerical simulations. The more important result, however, is the good agreement of the two distributions for the degenerate and for the non-degenerate empirical correlation matrices. We also mention that even the leading order deviations of the numerical simulations from the limiting distribution (81) seem to be approximately independent of the degree of the degeneracy  $l$  in the empirical correlation matrix.

The influence of the degeneracy in the empirical correlation matrix is strongest for the level density around the outliers, see the insets in Fig. 3. The reason was already discussed at the end of subsection IV A. The number of eigenvalues associated to each outlier is equal to the degeneracy, namely  $l$ . Hence, the shape of the distribution for each outlier strongly depends on  $l$ . However the mean value and the standard deviations of the distributions around the outliers should not change much with the degeneracy. To leading order we expect an independence which indeed is confirmed by the numerical simulations.

In Fig. 5 the cumulative distribution function  $\text{cdf}(t)$  is depicted. Being independent of the bin size, it provides a better measure than the distribution itself. The agreement with the analytical prediction of the positions (55) and

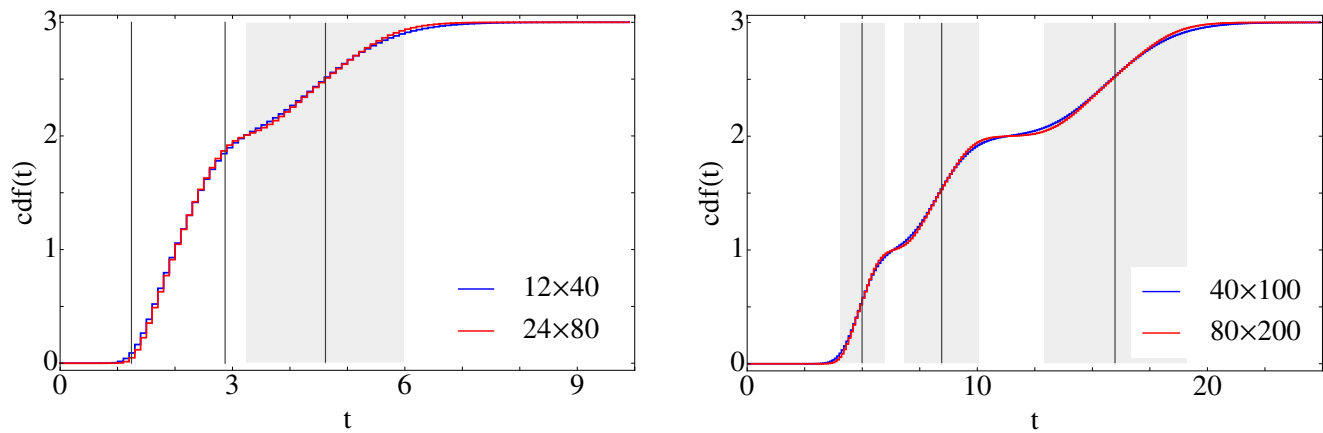


FIG. 5: Cumulative density functions  $\text{cdf}(t)$  around the three outliers for the real Wishart ensembles with the empirical correlation matrices shown in Fig. 2, for the time series  $T_{12 \times 40}$  (left) and  $T_{40 \times 100}$  (right). Blue and red histograms for the non-degenerate and degenerate empirical correlation matrices, respectively. Black vertical lines indicate the predicted positions (55) of the outliers and the grey shaded areas are the predicted fluctuations (57). The predicted fluctuations for the smallest outliers for the time series  $T_{12 \times 40}$  have imaginary values such that they have no grey shaded areas.

the fluctuations (57) for the three outliers is almost perfect for the set of the larger time series  $T_{40 \times 100}$  and thus seen to be independent of the degree of degeneracy. This also holds for the largest outlier in the case for the set of the smaller time series  $T_{12 \times 40}$ , while the two smaller outliers do not follow at all the analytical predictions. For the fluctuations of these two eigenvalues we find imaginary values with Eq. (57), indicating that the approximation discussed in subsection IV A fails. The reason becomes clear when looking at the inset of the left plot in Fig. 3. The two outliers overlap too much and even start to merge with the bulk. Hence, one has to modify the approximation presented in subsection IV A, as discussed below Eq. (58). Nonetheless the difference in the cumulative distributions of the outliers for the smaller and larger time series differ only marginally for the non-degenerate and degenerate case. This underlines our claim that even the outliers are in leading order unaffected by the (artificial) degeneracy.

## VI. CONCLUSIONS

Our study has produced three main results. The first one is that the spectral statistics of a real Wishart ensemble with a given empirical correlation matrix are independent of an artificially introduced degeneracy of the empirical eigenvalues. We derived this under moderate assumptions on the empirical correlation matrix and for an arbitrary degree of degeneracy. It holds for the local as well as for the macroscopic bulk statistics. Surprisingly, even the positions and the width of the fluctuations of possible outliers are independent of the degeneracy. The differences between the non-degenerate and the degenerate cases are the strongest close to the edges of the bulk and in the shape of the distribution around the outliers statistically significant differences between the non-degenerate and the degenerate cases emerge. We explained this behaviour theoretically and confirmed it with Monte-Carlo simulations.

The second main result is that the bulk and soft-edge statistics on the local scale of the mean level spacing follows the one of the Gaussian Orthogonal Ensemble (GOE). As we used the supersymmetry technique, we had to handle Efetov-Wegner boundary terms. We solved this problem employing Rothstein's theory and thereby exactly identified the statistics in the correlated real Wishart ensemble and in the GOE. Performing numerical simulations, we were able to compare the distribution of the largest and the smallest eigenvalue of the bulk with the Tracy-Widom distribution. The agreement is remarkably good even for small matrix dimensions.

Our third main result is a proposition, strongly corroborated by our analytical findings. As the degeneracies in the empirical correlation matrices do not influence the spectral statistics in a relevant fashion, we suggest to study the doubly degenerate case of an empirical correlation matrix instead of the non-degenerate one when one wishes to derive asymptotic analytical results for observables such as the distributions of individual eigenvalues and the level density. Due to the absence of square roots of determinants in the integrands, the doubly degenerate case is by far easier to treat than the non-degenerate one. As an example we employed results of Ref. [17] for the cumulative density function of the largest eigenvalue and derived an expression in terms of a Pfaffian in which all integrals are evaluated in closed form. We expect that other spectral observable can be asymptotically computed as well with this new method. Of course, for finite number and length of the time series this approach only yields an approximation, but our numerical

simulations indicate that these approximations are quite good even for relatively small matrix dimensions.

### Acknowledgments

We acknowledge support from the Deutsche Forschungsgemeinschaft, Sonderforschungsbereich TR12 (T.W. and T.G.), Sonderforschungsbereich 701 (M.K.) and the Alexander von Humboldt Foundation (M.K.). We considerably benefitted from the inspiring atmosphere at the conference “Random Matrix Theory: Foundations and Applications” in Cracow, Poland, where we started this project in July 2014.

### Appendix A: Rothstein’s Theory for Boundary Terms in Superanalysis

We consider an arbitrary diffeomorphism mapping one coordinate system  $(y, \eta)$  of a superspace to another one  $(x, \theta)$ . Here, we employ the notation of Rothstein [37], implying that  $(x, \theta)$  and  $(y, \eta)$  should not be confused with variables we use in the body of the paper. The transformation of an integral over an arbitrary superfunction  $f$  is not purely given by the Berezinian (Jacobian) but also incorporates corrections, henceforth abbreviated “b.t.”, the so called Efetov–Wegner boundary terms,

$$\int f(y, \eta) d[y, \eta] = \int f(y(x, \eta), \eta(x, \theta)) \text{sdet} \left( \frac{\partial(y, \eta)}{\partial(x, \theta)} \right) d[x, \theta] + \text{b.t.} \quad (\text{A1})$$

One can control these boundary terms by splitting the diffeomorphism into two steps. First we map the coordinate system to the numerical part  $y_0$  of  $y$  and to the first order part (in the Grassmann variables  $\theta$ )  $\eta_1$  of  $\eta$ . We denote the intermediate coordinates  $(x', \theta')$  such that

$$\int f(y, \eta) d[y, \eta] = \int f(y_0(x'), \eta_1(x', \theta')) \text{sdet} \left( \frac{\partial(y_0, \eta_1)}{\partial(x', \theta')} \right) d[x', \theta']. \quad (\text{A2})$$

This transformation is free of Efetov–Wegner boundary terms because  $y_0$  does not contain any Grassmann variables  $\theta$ . In the next step we can generate the remaining diffeomorphism by a vector field  $\hat{Y}(x, \theta)$  via  $(y(x, \eta), \eta(x, \theta)) = (y_0(x'(x, \eta)), \eta_1(x'(x, \eta), \theta'(x, \eta))) = \exp[\hat{Y}(x, \theta)](y_0(x), \eta_1(x, \theta))$  which yields the full transformation formula

$$\int f(y, \eta) d[y, \eta] = \int \exp[-\hat{Y}(x, \theta)] f(y_0(x), \eta_1(x, \theta)) \text{sdet} \left( \frac{\partial(y_0, \eta_1)}{\partial(x', \theta')} (x, \theta) \right) d[x, \theta]. \quad (\text{A3})$$

The correctness of this procedure was proven in [37, Chapter 3].

Two properties are known of the vector field  $\hat{Y}$ . First, it is a nilpotent vector field and a sum of even orders in the Grassmann variables. Thus the operator  $\exp[-\hat{Y}]$  is a finite sum of powers of  $\hat{Y}$  with the maximal power equal to half of the number of Grassmann variables. In our problem it would be  $2k^2$  and hence independent of the dimensions  $p$  and  $n$ . The second property of the vector field is that it only depends on the coordinate transformation and not on the integrand. We make use of this property in our calculation when identifying the  $k$ -point correlation function of the correlated Wishart ensemble with the sine kernel for the GOE.

- 
- [1] J. Wishart: *The generalised product moment distribution in samples from a normal multivariate population*, Biometrika A **20**, 32 (1928).
  - [2] E. P. Wigner: *On the statistical distribution of the widths and spacings of nuclear resonance levels*, Math. Proc. Cambridge **47**, 790 (1951).
  - [3] E. P. Wigner: *Random matrices in physics*, SIAM Review **9**,1 (1967).
  - [4] T. Guhr, A. Müller-Groeling, and H. A. Weidenmüller: *Random matrix theories in quantum physics: common concepts*, Phys. Rep. **299**, 189 (1998).
  - [5] F. J. Dyson: *The threefold way. algebraic structure of symmetry groups and ensembles in quantum mechanics*, J. Math. Phys. **3**, 1199 (1962).
  - [6] R. J. Muirhead: *Aspects of Multivariate Statistical Theory*, Wiley InterScience, New Jersey (2005).
  - [7] T. W. Anderson: *An Introduction to Multivariate Statistical Analysis*, 3rd ed., Wiley, New Jersey (2003).
  - [8] C. Chatfield: *The Analysis of Time Series: An Introduction*, 6th ed., Chapman and Hall/CRC Press, Boca Raton (2003).
  - [9] I. M. Johnstone: *High dimensional statistical inference and random matrices*, (2006) [arXiv:math/0611589].

- [10] P. Šeba: *Random matrix analysis of human EEG data*, Phys. Rev. Lett. **91**, 198104 (2003).
- [11] E. R. Pianka: *Evolutionary Ecology*, 7th ed., publisher Eric R. Pianka, (2011).
- [12] M. Feinberg: *Lectures on chemical reaction networks*, lecture notes (1979), URL: <https://crnt.osu.edu/LecturesOnReactionNetworks>
- [13] L. Laloux, P. Cizeau, J.-P. Bouchaud, and M. Potters: *Noise dressing of financial correlation matrices*, Phys. Rev. Lett. **83**, 1467 (1999) [arXiv:cond-mat/9810255].
- [14] V. Plerou, P. Gopikrishnan, B. Rosenow, L. A. N. Amaral, T. Guhr, and H. E. Stanley: *Random matrix approach to cross correlations in financial data*, Phys. Rev. E **65**, 066126 (2002) [arXiv:cond-mat/0108023].
- [15] Z. Bai and J.W. Silverstein, *Spectral Analysis of Large Dimensional Random Matrices*, Springer Series in Statistics, 2nd ed., Springer, Heidelberg (2010).
- [16] A. M. Tulino and S. Verdú: *Random Matrix Theory and Wireless Communications*, Foundations and Trends in Communications and Information Theory **1**, 1 (2004).
- [17] T. Wirtz, M. Kieburg, and T. Guhr: *Limiting statistics of the largest and smallest eigenvalues in the correlated Wishart model*, EPL **109**, 20005 (2015) [arXiv:1410.4719 [math-ph]].
- [18] Vinayak and A. Pandey Phys. Rev. **E81**, 036202 (2010)
- [19] C. Recher, M. Kieburg, and T. Guhr: *Eigenvalue density of real and complex Wishart correlation matrices*, Phys. Rev. Lett. **105**, 244101 (2010) [arXiv:1006.0812 [math-ph]].
- [20] C. Recher, M. Kieburg, T. Guhr, and M. R. Zirnbauer: *Supersymmetry approach to Wishart correlation matrices: Exact results*, J. Stat. Phys. **148**, 981 (2012) [arXiv:1012.1234 [math.ST]].
- [21] D. Waltner, T. Wirtz, and T. Guhr: *Eigenvalue density of the doubly correlated Wishart model: Exact results*, J. Phys. A **48**, 175204 (2014) [arXiv:math-ph/1412.3092].
- [22] T. Wirtz and T. Guhr: *Distribution of the smallest eigenvalue in the correlated Wishart model*, Phys. Rev. Lett. **111**, 094101 (2013) [arXiv:1306.4790 [math-ph]].
- [23] T. Wirtz and T. Guhr: *Distribution of the smallest eigenvalue in complex and real correlated Wishart ensembles*, J. Phys. A **47**, 075004 (2014) [arXiv:1310.2467 [math-ph]].
- [24] G. Akemann, T. Guhr, M. Kieburg, R. Wegner, and T. Wirtz: *Completing the picture for the smallest eigenvalue of real Wishart matrices*, Phys. Rev. Lett. **113**, 250201 (2014) [arXiv:1409.0360 [math-ph]].
- [25] T. Wirtz, G. Akemann, T. Guhr, M. Kieburg, and R. Wegner: *The Smallest Eigenvalue Distribution in the Real Wishart-Laguerre Ensemble with Even Topology*, J. Phys. A **48**, 245202 (2015) [arXiv:1502.03685 [math.PR]].
- [26] Y. V. Fyodorov, B. A. Khoruzhenko, and A. Nock: *Universal  $k$ -matrix distribution in  $\beta = 2$  ensembles of random matrices*, J. Phys. A **46**, 262001 (2013) [arXiv:1304.4368 [math-ph]].
- [27] Y. V. Fyodorov and A. Nock: *On random matrix averages involving half-integer powers of GOE characteristic polynomials*, [arXiv:math-ph/1410.5645] (2014) [arXiv:1410.5645 [math-ph]].
- [28] M. Zirnbauer: *Supersymmetry methods of random matrix theory*, published in Encyclopedia of Mathematical Physics, edited by J.-P. Francoise, G. L. Naber, and T. S. Tsun, Academic Press, Oxford (2006) [arXiv:math-ph/0404057].
- [29] T. Guhr: *Supersymmetry in random matrix theory*, published in “*The Oxford Handbook of Random Matrix Theory*”, edited by G. Akemann, J. Baik, and P. D. Francesco, Oxford University Press, Oxford (2011) [arXiv:1005.0979 [math-ph]].
- [30] V. A. Marčenko and L. A. Pastur: *Distribution of eigenvalues for some sets of random matrices*, Math. USSR-Sbornik **1**, 457 (1967).
- [31] J. Silverstein and S. Choi: *Analysis of the limiting spectral distribution of large dimensional random matrices*, J. Multi. Ana. **54**, 295 (1995).
- [32] Z. D. Bai and J. W. Silverstein: *No eigenvalues outside the support of the limiting spectral distribution of large-dimensional sample covariance matrices*, Ann. Prob. **26**, 316 (1998).
- [33] T. Shinzato: *Asymptotic Eigenvalue Distribution of Wishart Matrices whose Components are not Independently and Identically Distributed*, [arXiv:1605.06840 [q-fin.PM]] (2016).
- [34] G. Parisi and N. Sourlas: *Random Magnetic Fields, Supersymmetry, and Negative Dimensions*, Phys. Rev. Lett. **43**, 744 (1979).
- [35] F. Wegner: unpublished notes (1983).
- [36] K. Efetov: *Supersymmetry and theory of disordered metals*, Adv. Phys. **32**, 53 (1983).
- [37] M. Rothstein: *Integration on noncompact supermanifolds*, Trans. Am. Math. Soc. **299**, 387 (1987).
- [38] G. Akemann, M. Kieburg, and M. J. Phillips: *Skew-orthogonal Laguerre polynomials for chiral real asymmetric random matrices*, J. Phys. A **43**, 375207 (2010) [1005.2983 [math-ph]].
- [39] J. Verbaarschot, M. Zirnbauer, and H. Weidenmüller: *Grassmann integrations and stochastic quantum physics*, Phys. Rep. **129**, 367 (1985).
- [40] T. Guhr: *Dyson's correlation functions and graded symmetry*, J. Math. Phys. **32**, 336 (1991).
- [41] T. Guhr, *On the level density of coupled gaussian unitary ensembles*, Nucl. Phys. **A560**, 223 (1993).
- [42] F. Berezin: *Introduction to Superanalysis*, 1st ed., Reidel, Dordrecht (1987).
- [43] V. Kaymak, M. Kieburg, and T. Guhr: *The supersymmetry method for chiral random matrix theory with arbitrary rotation-invariant weights*, J. Phys. A **47**, 295201 (2014) [arXiv:1402.3458 [math-ph]].
- [44] M. R. Zirnbauer: *Riemannian symmetric superspaces and their origin in random matrix theory*, J. Math. Phys. **37**, 4986 (1996) [arXiv:math-ph/9808012].
- [45] H.-J. Sommers: *Superbosonization*, Acta Phys. Pol. B **38**, 4105 (2007) [arXiv:0710.5375 [cond-mat.stat-mech]].
- [46] P. Littellmann, H.-J. Sommers, and M. Zirnbauer: *Superbosonization of invariant random matrix ensembles*, Commun. Math. Phys. **283**, 343 (2008) [arXiv:0707.2929 [math-ph]].
- [47] F. Constantinescu: *The supersymmetric transfer matrix for linear chains with nondiagonal disorder*, J. Stat. Phys. **50**,

1167 (1988).

- [48] F. Constantinescu and H. F. de Groote: *Integral theorems for supersymmetric invariants*, J. Math. Phys. **30**, 981 (1989).
- [49] M. Kieburg, H. Kohler, and T. Guhr: *Integration of Grassmann variables over invariant functions on flat superspaces*, J. Math. Phys. **50**, 013528 (2009) [arXiv:0809.2674 [math-ph]].
- [50] T. Guhr: *Arbitrary Rotation Invariant Random Matrix Ensembles and Supersymmetry*, J. Phys. A **39**, 13191 (2006) [arXiv:math-ph/0606014].
- [51] M. Kieburg: *On the Efetov-Wegner terms by diagonalizing a Hermitian supermatrix*, J. Phys. A **44**, 285210 (2011) [arXiv:1011.0836 [math-ph]].
- [52] Z. Burda, A. Jarosz, G. Livan, M. A. Nowak, and A. Swiech: *Eigenvalues and Singular Values of Products of Rectangular Gaussian Random Matrices (The Extended Version)*, Acta Phys. Polon. B **42**, 939 (2011) [arXiv:1103.3964 [cond-mat.stat-mech]].
- [53] R. Speicher: *Free Probability Theory*, published in “*The Oxford Handbook of Random Matrix Theory*”, edited by G. Akemann, J. Baik, and P. D. Francesco, Oxford University Press, Oxford (2011) [arXiv:0911.0087 [math.PR]].
- [54] T. Pearcey: *The structure of an electromagnetic field in the neighbourhood of a cusp of a caustic*, Phil. Mag. **37**, 311 (1946).
- [55] E. Brézin and S. Hikami: *Universal singularity at the closure of a gap in a random matrix theory*, Phys. Rev. E **57**, 4140 (1998) [arXiv:cond-mat/9804023].
- [56] M. L. Mehta: *Random Matrices*, 3rd ed., Elsevier Academic Press, New York (2004).
- [57] M. L. Mehta: *A Note on Correlations between Eigenvalues of a Random Matrix*, Commun. Math. Phys. **20**, 245 (1971).
- [58] A. Borodin and C. D. Sinclair: *Correlation Functions of Asymmetric Real Matrices*, (2008) [arXiv:0706.2670v2[math-ph]]; *The Ginibre ensemble of real random matrices and its scaling limits*, Commun. Math. Phys. **291**, 177 (2009) [arXiv:0805.2986v1[math-ph]].
- [59] K. Johansson: *On Fluctuations of Eigenvalues of Random Hermitian Matrices*, Duke Math. Journ. **91**, 1 (1998).
- [60] C. Tracy and H. Widom: *On orthogonal and symplectic matrix ensembles*, Commun. Math. Phys. **177**, 727 (1996) [arXiv:solv-int/9509007].
- [61] M. Chiani: *Distribution of the largest eigenvalue for real Wishart and Gaussian random matrices and a simple approximation for the Tracy-Widom distribution*, J. Mult. Ana. **129**, 69 (2014) [arXiv:1209.3394 [cs.IT]].
- [62] A. E. Ingham: *An integral that occurs in statistics*, Proc. Camb. Phil. Soc. **29**, 271 (1933).
- [63] C. L. Siegel: *Über die analytische Theorie der quadratischen Formen I*, Ann. Math. **36**, 527 (1935).
- [64] M. Kieburg and T. Guhr: *A new approach to derive Pfaffian structures for random matrix ensembles*, J. Phys. A **43**, 135204 (2010) [arXiv:0912.0658 [math-ph]].